

Clustering microbiome data using mixtures of logistic normal multinomial models

Yuan Fang^{*} Sanjeena Subedi[†]

November 16, 2020

Abstract

Discrete data such as counts of microbiome taxa resulting from next-generation sequencing are routinely encountered in bioinformatics. Taxa count data in microbiome studies are typically high-dimensional, over-dispersed, and can only reveal relative abundance therefore being treated as compositional. Analyzing compositional data presents many challenges because they are restricted on a simplex. In a logistic normal multinomial model, the relative abundance is mapped from a simplex to a latent variable that exists on the real Euclidean space using the additive log-ratio transformation. While a logistic normal multinomial approach brings in flexibility for modeling the data, it comes with a heavy computational cost as the parameter estimation typically relies on Bayesian techniques. In this paper, we develop a novel mixture of logistic normal multinomial models for clustering microbiome data. Additionally, we utilize

^{*}Department of Mathematical Sciences, Binghamton University, State University of New York, 4400 Vestal Parkway East, Binghamton, NY, USA 13902. e: yfang8@binghamton.edu

[†]Department of Mathematical Sciences, Binghamton University, State University of New York, 4400 Vestal Parkway East, Binghamton, NY, USA 13902. e: sdang@binghamton.edu

an efficient framework for parameter estimation using variational Gaussian approximations (VGA). Adopting a variational Gaussian approximation for the posterior of the latent variable reduces the computational overhead substantially. The proposed method is illustrated on simulated and real datasets.

Keywords: Clustering, Model-based clustering, logistic normal multinomial, Microbiome data, Variational Gaussian approximation

1 Introduction

The human microbiome comprises of complex communities of microorganisms including but not limited to bacteria, fungi, and viruses, that inhabit in and on a human body (Morgan and Huttenhower, 2012; Li, 2015). It is estimated that there are approximately 10^{14} microbial cells associated with the human body, which is around 10 times the number of human cells (Ley et al., 2006; Fraher et al., 2012). The human microbiome plays a significant role in human health and disease status. There is evidence indicating that microbial dysbiosis may lead to diseases such as cardiovascular diseases (Koeth et al., 2013), diabetes (Qin et al., 2012), inflammatory bowel disease (Greenblum et al., 2012), obesity (Turnbaugh et al., 2009), and many others. Next generation sequencing techniques, such as the 16S ribosomal RNA (rRNA) amplicon sequencing or shotgun metagenomics sequencing, provide an effective way for quantification and comparison of the bacterial composition, including types and abundance of different bacteria within biological samples (Streit and Schmitz, 2004; Kuczynski et al., 2012; Yatsunenko et al., 2012; Äijö et al., 2018). In 16S rRNA sequencing, the 16S rRNA, which is ubiquitous in all bacterial organisms but it also has distinct variable regions that can be used to discriminate between different bacteria is first PCR-amplified and then sequenced (Kuczynski et al., 2012). Shotgun sequencing on the other hand is an

untargeted sequencing of all microbial genomes in a sample (Quince et al., 2017). In either case, short reads are preprocessed through steps of quality control and filtering steps. The processed raw sequence reads are then clustered into operational taxonomic units (OTUs) at a certain similarity level (Eckburg et al., 2005) where each OTU is characterized by a representative DNA sequence that could be assigned to a taxonomic lineage by comparing to a known database (Li, 2015). Resulting read counts at different taxonomic levels for n samples over $K + 1$ taxa are stored as a $n \times (K + 1)$ matrix \mathbf{W} , with the entry $W[i, k]$ representing the counts recorded for the k^{th} taxon in the i^{th} sample.

Statistical analysis of microbiome data is complicated. The microbiome count data can only reveal relative abundance, i.e., the abundance for each taxa are constrained by the total sum of the microbes in that particular sample and the total sum of microbes could vary among the samples depending on the sequencing depth. Different individuals could share various communities of microorganisms, with only a few major ones in common, and even for one person, the microbial composition could be totally different in different body sites. The heterogeneity of the microbiome samples also leads to over-dispersion. See Hamady and Knight (2009) for a detailed review of challenges related to analyzing microbiome data. Standard multivariate analysis usually fails to capture these properties of the microbiome data. Different models have been proposed for the microbiome counts in the literature that capture one or more of the above intrinsic characteristics such as the negative binomial model (Zhang et al., 2017), zero-inflated negative binomial model (Zhang and Yi, 2020), zero-inflated Poisson model (Joseph et al., 2013; Xu et al., 2020), Dirichlet-multinomial model (Holmes et al., 2012; Chen and Li, 2013; Subedi et al., 2020), and the logistic normal multinomial model (Xia et al., 2013). While modelling such count data, a negative binomial (NB) model can allow for the variance to be larger than the mean using a dispersion parameter, thus handling over-dispersion better than a simple Poisson model. The zero-inflated negative binomial (ZINB)

and zero-inflated Poisson (ZIP) have been proposed to account for excessive number of zeros (Joseph et al., 2013). Xu et al. (2015) provides a comparison among the zero-inflated models. However, the NB and ZINB model ignore the compositional nature of these microbial counts. Chen and Li (2013), Holmes et al. (2012), Wadsworth et al. (2017) and Subedi et al. (2020) utilized the Dirichlet-multinomial model for microbial counts that takes into account the compositional nature of these data. Alternately, Xia et al. (2013) employed the logistic normal multinomial model, mapping the relative abundance from a simplex to a latent variable that exists on the real Euclidian space using the additive log-ratio transformation. Cao et al. (2017) exploited a Poisson-multinomial model and performed a multi-sample estimation of microbial composition in positive simplex space from a high-dimensional sparse count table. Caporaso et al. (2011) quantified variations of microbial composition across time by projecting the dynamics using low-dimensional embedding. Äijö et al. (2018) proposed a temporal probabilistic model for the microbiome composition using a hierarchical multinomial model. Silverman et al. (2018) also developed a dynamic linear model based on the logistic normal multinomial model to study the artificial human guts microbiome.

Clustering microbiome samples into groups that share similar microbial compositional patterns is of great interest (Holmes et al., 2012). Clustering algorithms are usually categorized into hierarchical clustering and distance-based clustering. Hierarchical clustering has been applied for clustering microbiome data, yet it requires the choice of a cut-off threshold, according to which samples can be divided into groups (Holmes et al., 2012). On the other hand, k -means clustering, a distance-based method, might not be appropriate for microbiome compositions because it is typically used for continuous data and obtains spherical clusters. Hence, model-based clustering approaches that utilize a finite mixture model have been widely used in the last decade to cluster microbiome data (Holmes et al., 2012; Subedi et al., 2020). A finite mixture model assumes that the population consists of a finite

mixture of subpopulations (or clusters), each represented by a known distribution (McLachlan and Peel, 2000; Zhong and Ghosh, 2003; Frühwirth-Schnatter, 2006; McNicholas, 2016). Due to the flexibility in choosing component distributions to model different type of data, several mixture models based on discrete distributions have been developed to study count data, especially, for gene expression data. Rau et al. (2011) proposed a clustering approach for RNA-seq data using mixtures of univariate Poisson distributions; Papastamoulis et al. (2016) proposed a mixture of Poisson regression models; Si et al. (2014) studied model-based clustering for RNA-seq data using a mixture of negative binomial (NB) distributions; Silva et al. (2019) proposed a multivariate Poisson-log normal mixture model for clustering gene expression data. However, due to the compositional nature of microbiome data, none of the about discrete mixture models can be employed directly for clustering microbiome data. Holmes et al. (2012) adopted the Dirichlet-multinomial (DM) model, where the underlying compositions are modeled as a Dirichlet prior to a multinomial distribution that describes the taxa counts, and proposed a mixture of DM models to cluster samples.

In this paper, we develop a model-based clustering approach using the logistic normal multinomial model proposed by Xia et al. (2013) to cluster microbiome data. In the logistic normal multinomial model, the observed counts are modeled using a multinomial distribution, and the relative abundance is regarded a random vector on a simplex, which is further mapped to a latent variable that exists on the real Euclidean space through an additive log-ratio transformation. While this approach captures the additional variability compared to a multinomial model, it does not possess a closed form expression of the log-likelihood functions and of the posterior distributions of the latent variables. Therefore, the expected complete-data log-likelihoods needed in the E-step of a traditional EM algorithm are usually intractable. In such a scenario, one commonly used approach is a variant of the EM algorithm that relies on Bayesian techniques using Markov chain Monte Carlo (MCMC); however, this

would typically bring in high computational cost. Here, we develop a variant of the EM algorithm, here on referred to as a variational EM algorithm for parameter estimation that utilizes variational Gaussian approximations (VGA). In Variational Gaussian approximations (VGA; Barber and Bishop, 1998), a complex posterior distribution is approximated using computationally convenient Gaussian densities by minimizing the Kullback-Leibler (KL) divergence between the true and the approximating densities (Bishop, 2006; Arridge et al., 2018). Adopting a variational Gaussian approximation delivers accurate approximations of the complex posterior while reducing computational overhead substantially. Hence, this approach has become extremely popular in many different fields in machine learning. (Barber and Bishop, 1998; Bishop, 2006; Archambeau et al., 2007; Khan et al., 2012; Challis and Barber, 2013; Blei et al., 2017).

The contribution of the paper is two folds - first, we develop a computationally efficient framework for parameter estimation for logistic normal multinomial model through the use of variational Gaussian approximations and second, we utilize this framework to develop a model-based clustering framework for clustering microbiome data. Through simulations and applications to microbiome data, the utilities of the proposed approach is illustrated. The paper is structured as follows: Section 2 describes the logistic normal multinomial model for microbiome count data and details the variational Gaussian approximations. Section 2.3 provides a mixture model framework based on the model described in Section 2 together with a variational EM algorithm for parameter estimation. In Section 3, clustering results are illustrated by applying the proposed algorithm on both simulated and real data. Finally, discussion on the advantages and limitations along with some future directions are provided in Section 4.

2 Methodology

2.1 The logistic normal multinomial model for microbiome compositional data

Suppose we have $K + 1$ bacterial taxa for a sample denoted as a random vector $\mathbf{W} = (W_1, \dots, W_{K+1})^\top$. Here, the taxa could represent any level of the bacterial phylogeny such as OTU, species, genus, phylum, etc. Due to the fact that taxa counts from 16S sequencing can only reveal relative abundance, let's suppose there is a vector $\boldsymbol{\Theta} = (\Theta_1, \dots, \Theta_{K+1})$ such that $\sum_{k=1}^{K+1} \Theta_k = 1$, which represents the underlying composition of the bacterial taxa. Then, the microbial taxa count \mathbf{W} can be modeled as a multinomial random variable with the following conditional density function:

$$p(\mathbf{w}|\boldsymbol{\Theta}) \propto \prod_{k=1}^{K+1} (\Theta_k)^{w_k}.$$

Several models have been proposed in the literature that capture the relative abundance nature of microbiome data and analyze the compositional data (Holmes et al., 2012; Xia et al., 2013). Here we use the model by Xia et al. (2013) that utilizes an additive log-ratio transformation $\phi(\boldsymbol{\Theta})$ proposed by Aitchison (1982) such that:

$$\mathbf{Y} = \phi(\boldsymbol{\Theta}) = \left(\log \left(\frac{\Theta_1}{\Theta_{K+1}} \right), \dots, \log \left(\frac{\Theta_K}{\Theta_{K+1}} \right) \right)^\top. \quad (1)$$

This transformation ϕ maps the vector $\boldsymbol{\Theta}$ from a K -dimensional simplex to the K -dimensional real space \mathbb{R}^K while \mathbf{Y} is assumed to follow a multivariate normal distribution with mean $\boldsymbol{\mu}$

and covariance Σ with the density function

$$p(\mathbf{y}|\boldsymbol{\mu}, \Sigma) \propto |\Sigma|^{-\frac{1}{2}} \exp \left\{ -\frac{1}{2}(\mathbf{y} - \boldsymbol{\mu})^\top \Sigma^{-1}(\mathbf{y} - \boldsymbol{\mu}) \right\}.$$

As this additive log-ratio transformation is a one-to-one map, the inverse operator of ϕ exists and is given by

$$\boldsymbol{\Theta} = \phi^{-1}(\mathbf{Y}) = \begin{cases} \frac{\exp(Y_k)}{1 + \sum_{k=1}^K \exp(Y_k)} & k = 1, \dots, K \\ \frac{1}{1 + \sum_{k=1}^K \exp(Y_k)} & k = K + 1 \end{cases}.$$

Hence, the joint density of \mathbf{W} and \mathbf{Y} up to a constant is as follows:

$$p(\mathbf{w}, \mathbf{y}) \propto p(\mathbf{w}|\phi^{-1}(\mathbf{y})) p(\mathbf{y}|\boldsymbol{\mu}, \Sigma) = \prod_{k=1}^{K+1} (\phi^{-1}(\mathbf{y})_k)^{w_k} \times |\Sigma|^{-\frac{1}{2}} \exp \left\{ -\frac{1}{2}(\mathbf{y} - \boldsymbol{\mu})^\top \Sigma^{-1}(\mathbf{y} - \boldsymbol{\mu}) \right\}.$$

2.2 A variational Gaussian lower bound

For the microbiome data, only the count vector \mathbf{W} are observed while the latent variable \mathbf{Y} is unobserved. The marginal density of \mathbf{W} can be written as

$$p(\mathbf{w}) = \int_{\mathbb{R}^K} p(\mathbf{w}, \mathbf{y}) d\mathbf{y} \propto \int_{\mathbb{R}^K} \prod_{k=1}^{K+1} (\phi^{-1}(\mathbf{y})_k)^{w_k} \times |\Sigma|^{-\frac{1}{2}} \exp \left\{ -\frac{1}{2}(\mathbf{y} - \boldsymbol{\mu})^\top \Sigma^{-1}(\mathbf{y} - \boldsymbol{\mu}) \right\} d\mathbf{y}.$$

Note that this marginal distribution of \mathbf{W} involves multiple integrals and cannot be further simplified. Here, in presence of missing data, an expectation-maximization algorithm (Dempster et al., 1977) or some variant of it is typically utilized for parameter estimation. An EM-algorithm comprises two steps: an E-step in which the expected value of the complete data (i.e. observed and missing data) log-likelihood is computed given the observed data and current parameter estimate and an M-step in which the complete data log-likelihood

is maximized. These steps are repeated until convergence to obtain the maximum likelihood estimate of the parameters. To compute the expected value of the complete data log-likelihood, $\mathbb{E}(\mathbf{Y} \mid \mathbf{w})$ and $\mathbb{E}(\mathbf{Y}\mathbf{Y}^T \mid \mathbf{w})$ needs to be computed for which we need $p(\mathbf{y}|\mathbf{w})$. Mathematically,

$$p(\mathbf{y}|\mathbf{w}) = \frac{p(\mathbf{w}, \mathbf{y})}{p(\mathbf{w})} = \frac{\prod_{k=1}^{K+1} (\phi^{-1}(\mathbf{y})_k)^{w_k} \times |\Sigma|^{-\frac{1}{2}} \exp \left\{ -\frac{1}{2}(\mathbf{y} - \boldsymbol{\mu})^\top \Sigma^{-1}(\mathbf{y} - \boldsymbol{\mu}) \right\}}{\int_{\mathbb{R}^K} \prod_{k=1}^{K+1} (\phi^{-1}(\mathbf{y})_k)^{w_k} \times |\Sigma|^{-\frac{1}{2}} \exp \left\{ -\frac{1}{2}(\mathbf{y} - \boldsymbol{\mu})^\top \Sigma^{-1}(\mathbf{y} - \boldsymbol{\mu}) \right\} d\mathbf{y}}.$$

However, the denominator involves multiple integrals and cannot be further simplified. One could employ a Markov chain Monte Carlo (MCMC) approach to explore the posterior state space; however, these methods are typically computationally expensive, especially for high-dimensional problems. Here, we propose the use of variational Gaussian approximation (VGA; Barber and Bishop, 1998) for parameter estimation. A VGA aims to find an optimal and tractable approximation that has a Gaussian parametric form to approximate the true complex posterior by minimizing the Kullback-Leibler divergence between the true and the approximating densities. It has been successfully used in many practical applications to overcome this challenge (Bishop, 2006; Archambeau et al., 2007; Wainwright et al., 2008; Khan et al., 2012; Challis and Barber, 2013; Arridge et al., 2018). In order to utilize VGA, we define a new latent variable $\boldsymbol{\eta}$ by transforming \mathbf{Y} such that

$$\boldsymbol{\eta} = B\mathbf{Y}, \quad \text{where } B = \begin{pmatrix} 1 & 0 & \dots & 0 \\ 0 & 1 & \dots & 0 \\ \vdots & \vdots & \dots & \vdots \\ 0 & 0 & \dots & 1 \\ 0 & 0 & \dots & 0 \end{pmatrix}, \quad (2)$$

is a $(K + 1) \times K$ matrix which takes the form as an identity matrix attached by a row of K zeros. Given that $\mathbf{Y} \sim \mathcal{N}(\boldsymbol{\mu}, \boldsymbol{\Sigma})$, the new latent variable $\boldsymbol{\eta} \sim \mathcal{N}(\tilde{\boldsymbol{\mu}}, \tilde{\boldsymbol{\Sigma}})$ where

$$\tilde{\boldsymbol{\mu}} = B\boldsymbol{\mu} = (\boldsymbol{\mu}, 0)^\top; \quad \tilde{\boldsymbol{\Sigma}} = B\boldsymbol{\Sigma}B^\top = \left(\begin{array}{c|c} \boldsymbol{\Sigma} & \mathbf{0}_{K \times 1} \\ \hline \mathbf{0}_{1 \times K} & 0 \end{array} \right). \quad (3)$$

Then, the underlying composition variable $\boldsymbol{\Theta}$ can be written as a function of $\boldsymbol{\eta}$:

$$\boldsymbol{\Theta} = \tilde{\phi}^{-1}(\boldsymbol{\eta}) = \frac{\exp \eta_k}{\sum_{k=1}^{K+1} \exp \eta_k} k = 1 \dots, K + 1. \quad (4)$$

Suppose we have an approximating density $q(\boldsymbol{\eta})$, then the marginal log density of \mathbf{W} can be written as:

$$\begin{aligned} \log p(\mathbf{w}) &= \int \log p(\mathbf{w}) q(\boldsymbol{\eta}) d\boldsymbol{\eta} \\ &= \int \log \frac{p(\mathbf{w}, \boldsymbol{\eta})/q(\boldsymbol{\eta})}{p(\boldsymbol{\eta} | \mathbf{w})/q(\boldsymbol{\eta})} q(\boldsymbol{\eta}) d\boldsymbol{\eta} \\ &= \int [\log p(\mathbf{w}, \boldsymbol{\eta}) - \log q(\boldsymbol{\eta})] q(\boldsymbol{\eta}) d\boldsymbol{\eta} + \int \log \frac{q(\boldsymbol{\eta})}{p(\boldsymbol{\eta} | \mathbf{w})} q(\boldsymbol{\eta}) d\boldsymbol{\eta} \\ &= F(q(\boldsymbol{\eta}), \mathbf{w}) + D_{KL}(q||p), \end{aligned}$$

where the first part $F(q(\boldsymbol{\eta}), \mathbf{w}) = \int q(\boldsymbol{\eta}) \log \frac{p(\mathbf{w}, \boldsymbol{\eta})}{q(\boldsymbol{\eta})} d\boldsymbol{\eta}$ is called the evidence lower bound (ELBO; Barber and Bishop, 1998) and the second part $D_{KL}(q||p) = \int \log \frac{q(\boldsymbol{\eta})}{p(\boldsymbol{\eta} | \mathbf{w})} q(\boldsymbol{\eta}) d\boldsymbol{\eta}$ is the Kullback-Leibler divergence from $p(\boldsymbol{\eta} | \mathbf{w})$ to $q(\boldsymbol{\eta})$. Hence, minimizing the Kullback-Leibler divergence is equivalent to maximizing the following evidence lower bound (ELBO).

In VGA, we assume $q(\boldsymbol{\eta})$ is a Gaussian distribution, such that

$$q(\boldsymbol{\eta}) = \mathcal{N}(\boldsymbol{\eta} | \mathbf{m}, V) \propto |V|^{-\frac{1}{2}} \exp \left\{ -\frac{1}{2} (\boldsymbol{\eta} - \mathbf{m})^\top V^{-1} (\boldsymbol{\eta} - \mathbf{m}) \right\}.$$

Given the fact that $q(\boldsymbol{\eta})$ is fully characterized by its mean vector and covariance matrix, the above lower bound is a function of the variational parameters \mathbf{m} and V and we aim to find the optimal set of (\mathbf{m}, V) such that it maximizes $F(q(\boldsymbol{\eta}, \mathbf{w}))$. $F(q(\boldsymbol{\eta}, \mathbf{w}))$ can be separated into three parts:

$$F(q(\boldsymbol{\eta}), \mathbf{w}) = F(\mathbf{m}, V) = - \int q(\boldsymbol{\eta}) \log q(\boldsymbol{\eta}) d\boldsymbol{\eta} + \int q(\boldsymbol{\eta}) \log p(\boldsymbol{\eta}) d\boldsymbol{\eta} + \int q(\boldsymbol{\eta}) \log p(\mathbf{w}|\boldsymbol{\eta}) d\boldsymbol{\eta}.$$

Up to a constant, the last integral, which is denoted as γ , in the above decomposition is given as follows:

$$\begin{aligned} \gamma &= \int q(\boldsymbol{\eta}) \log p(\mathbf{w}|\boldsymbol{\eta}) d\boldsymbol{\eta} \\ &= \mathbb{E}_{q(\boldsymbol{\eta}|\mathbf{m}, V)} \left[\mathbf{w}^\top \boldsymbol{\eta} - \sum_{k=1}^{K+1} w_k \log \left(\sum_{k=1}^{K+1} \exp \eta_k \right) \right] \\ &= \mathbf{w}^\top \mathbf{m} - \left(\sum_{k=1}^{K+1} w_k \right) \mathbb{E}_{q(\boldsymbol{\eta}|\mathbf{m}, V)} \left[\log \left(\sum_{k=1}^{K+1} \exp \eta_k \right) \right]. \end{aligned}$$

Similar to Blei and Lafferty (2006), we use an upper bound for the expectation of log sum exponential term with a Taylor expansion,

$$\mathbb{E}_{q(\boldsymbol{\eta}|\mathbf{m}, V)} \left[\log \left(\sum_{k=1}^{K+1} \exp \eta_k \right) \right] \leq \xi^{-1} \left\{ \sum_{k=1}^{K+1} \mathbb{E}_{q(\boldsymbol{\eta}|\mathbf{m}, V)} [\exp(\eta_k)] \right\} - 1 + \log(\xi),$$

where $\xi \in \mathbb{R}$ is introduced as a new variational parameter.

Here, we further assume that V is a diagonal matrix with the first K diagonal element of V as v_k^2 and the $K+1^{th}$ diagonal element is set to 0 such that

$$v_k^2 = \begin{cases} v_k^2, & k = 1, \dots, K \\ 0, & k = K+1. \end{cases}$$

We also denote the k -th element of \mathbf{m} as m_k such that

$$m_k = \begin{cases} m_k, & k = 1, \dots, K \\ 0, & k = K + 1. \end{cases}$$

Hence, the expectation

$$\mathbb{E}_{q(\boldsymbol{\eta}|\mathbf{m}, V)} [\exp(\eta_k)] = \exp\left(m_k + \frac{v_k^2}{2}\right), \text{ for } k = 1, \dots, K + 1.$$

Based on this upper bound, we obtain a concave lower bound to γ and to the ELBO. The new concave variational Gaussian lower bound to the model evidence $\log p(\mathbf{w})$ is given as follows

$$\begin{aligned} \tilde{F}(\mathbf{m}, V, \tilde{\boldsymbol{\mu}}, \tilde{\boldsymbol{\Sigma}}, \xi) &= \mathbf{w}^\top \mathbf{m} - \left(\sum_{k=1}^{K+1} w_k \right) \left\{ \xi^{-1} \left[\sum_{k=1}^{K+1} \exp\left(m_k + \frac{v_k^2}{2}\right) \right] - 1 + \log(\xi) \right\} \\ &\quad - \frac{1}{2} \log |B^\top \tilde{\boldsymbol{\Sigma}} B| - \frac{1}{2} (\mathbf{m} - \tilde{\boldsymbol{\mu}})^\top \tilde{\boldsymbol{\Sigma}}^* (\mathbf{m} - \tilde{\boldsymbol{\mu}}) - \frac{1}{2} \text{Tr}(\tilde{\boldsymbol{\Sigma}}^* V) \\ &\quad + \frac{1}{2} \sum_{k=1}^K \log(v_k^2) + \frac{K}{2}, \end{aligned} \tag{5}$$

where

$$\tilde{\boldsymbol{\Sigma}}^* = \left(\begin{array}{c|c} \boldsymbol{\Sigma}^{-1} & \mathbf{0}_{K \times 1} \\ \hline \mathbf{0}_{1 \times K} & 0 \end{array} \right),$$

is the generalized inverse of $\tilde{\boldsymbol{\Sigma}}$. Details on the derivation of this lower bound can be found in Appendix A. Given fixed \mathbf{w} , $\tilde{\boldsymbol{\mu}}$, and $\tilde{\boldsymbol{\Sigma}}$, this lower bound only depends on the variational parameter set (\mathbf{m}, V, ξ) .

Maximization of the lower bound $\tilde{F}(\mathbf{m}, V, \tilde{\boldsymbol{\mu}}, \tilde{\boldsymbol{\Sigma}}, \xi)$ with respect to ξ has a closed form

solution and is given by

$$\hat{\xi} = \sum_{k=1}^{K+1} \exp \left(m_k + \frac{v_k^2}{2} \right). \quad (6)$$

However, maximization with respect to \mathbf{m} and $v_k, k = 1, \dots, K$ do not possess analytical solutions. We use Newton's method to search for roots to the following derivatives:

$$\frac{\partial \tilde{F}}{\partial \mathbf{m}} = \mathbf{w} - \tilde{\Sigma}^* (\mathbf{m} - \tilde{\boldsymbol{\mu}}) - \left(\sum_{k=1}^{K+1} w_k \right) \xi^{-1} \exp \left(\mathbf{m} + \frac{\mathbf{v}^2}{2} \right), \quad (7)$$

with $\mathbf{v}^2 = (v_1^2, \dots, v_K^2, 0)$ denoting the diagonal element of V as a vector; and

$$\frac{\partial \tilde{F}}{\partial v_k} = v_k^{-1} - v_k \tilde{\Sigma}_{k,k}^* - \left(\sum_{k=1}^{K+1} w_k \right) \xi^{-1} \exp \left(m_k + \frac{v_k^2}{2} \right) v_k. \quad (8)$$

Details can be found in Appendix A.

2.3 Mixture of logistic normal multinomial models

Assume there are G subgroups in the population, with π_g denoting the mixing weight of the g -th component such that $\sum_{g=1}^G \pi_g = 1$. Then, a G -component finite mixtures logistic normal multinomial models can be written as

$$f(\mathbf{w} \mid \boldsymbol{\vartheta}) = \sum_{g=1}^G \pi_g f_g(\mathbf{w} \mid \boldsymbol{\vartheta}_g),$$

where $f_g(\mathbf{w} \mid \boldsymbol{\vartheta}_g)$ represents the density function of the observation $\mathbf{W} = \mathbf{w}$, given that \mathbf{W} comes from the g -th component with parameters $\boldsymbol{\vartheta}_g$.

Provided n observed counts, $\mathbf{w} = (\mathbf{w}_1, \dots, \mathbf{w}_n)$ with a transformed underlying the com-

position $\mathbf{Y}_i, i = 1, \dots, n$, the likelihood of a G -component finite mixture is given as

$$\mathcal{L}(\boldsymbol{\vartheta} \mid \mathbf{w}) = \prod_{i=1}^n f(\mathbf{w}_i \mid \boldsymbol{\vartheta}) = \prod_{i=1}^n \sum_{g=1}^G \pi_g f_g(\mathbf{w}_i \mid \vartheta_g) = \prod_{i=1}^n \sum_{g=1}^G \pi_g \int p(\mathbf{w}_i \mid \mathbf{y}_i) p(\mathbf{y}_i \mid \vartheta_g) d\mathbf{y}_i.$$

In clustering, the unobserved component membership is denoted by an indicator variable $z_{ig}, i = 1, \dots, n, g = 1, \dots, G$ that takes the form

$$z_{ig} = \begin{cases} 1 & \text{if the } i\text{-th observation is from the } g\text{-th group,} \\ 0 & \text{otherwise.} \end{cases}$$

Therefore, conditional on z_{ig} , we have

$$\mathbf{Y}_i \mid z_{ig} = 1 \sim \mathcal{N}(\boldsymbol{\mu}_g, \boldsymbol{\Sigma}_g).$$

In order to utilize the variational approach for parameter estimation, we again define a new latent variable $\boldsymbol{\eta}$ such that $\boldsymbol{\eta} = B\mathbf{Y}$ and

$$\boldsymbol{\eta}_i \mid z_{ig} = 1 \sim \mathcal{N}(\tilde{\boldsymbol{\mu}}_g, \tilde{\boldsymbol{\Sigma}}_g), \text{ where } \tilde{\boldsymbol{\mu}}_g = B\boldsymbol{\mu}_g = (\boldsymbol{\mu}_g, 0)^\top \text{ and } \tilde{\boldsymbol{\Sigma}}_g = B\boldsymbol{\Sigma}_g B^\top = \left(\begin{array}{c|c} \boldsymbol{\Sigma}_g & \mathbf{0}_{K \times 1} \\ \hline \mathbf{0}_{1 \times K} & 0 \end{array} \right).$$

Therefore, the complete data (i.e., observed counts \mathbf{W} and unobserved class label indicator variable) log-likelihood using the marginal density of \mathbf{W} is

$$\ell = \log \left[\prod_{i=1}^n \prod_{g=1}^G \pi_g f_g(\mathbf{w}_i \mid \vartheta_g) \right]^{z_{ig}} = \sum_{i=1}^n \sum_{g=1}^G z_{ig} \left\{ \log \pi_g + \log \left[\int p(\mathbf{w}_i \mid \boldsymbol{\eta}_i) p(\boldsymbol{\eta}_i \mid \tilde{\boldsymbol{\mu}}_g, \tilde{\boldsymbol{\Sigma}}_g) d\boldsymbol{\eta}_i \right] \right\}.$$

To perform variational inference on the mixture model, we substitute $\log \left[\int p(\mathbf{w}_i \mid \boldsymbol{\eta}_i) p(\boldsymbol{\eta}_i \mid \boldsymbol{\mu}_g, \boldsymbol{\Sigma}_g) d\boldsymbol{\eta}_i \right]$ by the variational Gaussian lower bound $\tilde{F}(\mathbf{m}, V, \tilde{\boldsymbol{\mu}}, \tilde{\boldsymbol{\Sigma}}, \xi)$ derived in Section 2.2. Hence,

the variational Gaussian lower bound of complete data log likelihood can be written as:

$$\begin{aligned}
\tilde{\mathcal{L}} = & \sum_{i=1}^n \sum_{g=1}^G z_{ig} \log \pi_g + \sum_{i=1}^n \sum_{g=1}^G z_{ig} \mathbf{w}_i^\top \mathbf{m}_{ig} \\
& - \sum_{i=1}^n \sum_{g=1}^G z_{ig} \left(\sum_{k=1}^{K+1} w_{ik} \right) \left\{ \xi_i^{-1} \left[\sum_{k=1}^{K+1} \exp \left(m_{igk} + \frac{v_{igk}^2}{2} \right) \right] - 1 + \log(\xi_i) \right\} \\
& + \sum_{i=1}^n \sum_{g=1}^G z_{ig} \left\{ \frac{1}{2} \log |B^\top \tilde{\Sigma}_g B| - \frac{1}{2} (\mathbf{m}_{ig} - \tilde{\boldsymbol{\mu}}_g)^\top \tilde{\Sigma}_g^* (\mathbf{m}_{ig} - \tilde{\boldsymbol{\mu}}_g) \right. \\
& \quad \left. - \frac{1}{2} \text{Tr}(\tilde{\Sigma}_g^* V_{ig}) + \frac{1}{2} \sum_{k=1}^K \log(v_{igk}^2) + \frac{K}{2} \right\}.
\end{aligned} \tag{9}$$

Hence, we need to find optimal solutions to variational parameters $(\mathbf{m}_{ig}, V_{ig}, \xi_i)$ that are associated with each observation $\mathbf{w}_i, i = 1, \dots, n$, as well as the model group-specific Gaussian parameters $(\tilde{\boldsymbol{\mu}}_g, \tilde{\Sigma}_g), g = 1, \dots, G$, such that the complete data variational Gaussian lower bound $\tilde{\mathcal{L}}$ is maximized. The use of VGA provides great reduction in the computational time. Äijö et al. (2018) who utilize an MCMC based approach state that “*It takes approximately an hour on a modern laptop to analyze a dataset of 160 taxa and 27 time points*”. In a clustering context, an equivalent step needs to be computed at every iteration of the expectation-maximization algorithm and the number of iterations required for the analysis is typically in hundreds. An equivalent step in each iteration of the clustering framework for the same size simulated dataset can be run in 0.83 seconds. This drastically reduces the computational overhead making it feasible to extend these models for clustering in a high dimensional setting.

2.4 The variational EM algorithm

Parameter estimation can be done in an iterative EM-type approach, from here on referred to as variational EM such that the following steps are iterated until convergence. For the

parameters that do not have a closed form solution to the optimization, we perform one step of Newton's method to approximate the root to their first derivatives.

Step 1: Conditional on the variational parameters $(\mathbf{m}_{ig}, V_{ig}, \xi_i)$ and model group-specific Gaussian parameters $(\tilde{\boldsymbol{\mu}}_g, \tilde{\boldsymbol{\Sigma}}_g)$, $\mathbb{E}(Z_{ig} \mathbf{W}_i)$ is computed. Given $(\tilde{\boldsymbol{\mu}}_g, \tilde{\boldsymbol{\Sigma}}_g)$,

$$\mathbb{E}(Z_{ig} \mid \mathbf{w}_i) = \frac{\pi_g f_g(\mathbf{w}_i \mid \tilde{\boldsymbol{\mu}}_g, \tilde{\boldsymbol{\Sigma}}_g)}{\sum_{h=1}^G \pi_h f_h(\mathbf{w}_i \mid \tilde{\boldsymbol{\mu}}_h, \tilde{\boldsymbol{\Sigma}}_h)}.$$

This involves the marginal distribution of \mathbf{W} and hence, we use an approximation of $\mathbb{E}(Z_{ig} \mid \mathbf{w}_i)$ where we replace the marginal density \mathbf{W} by the exponent of ELBO such that

$$\hat{z}_{ig} := \frac{\pi_g \exp \left\{ \tilde{F} \left(\mathbf{w}_i, \mathbf{m}_{ig}, V_{ig}, \tilde{\boldsymbol{\mu}}_g, \tilde{\boldsymbol{\Sigma}}_g, \xi_i \right) \right\}}{\sum_{j=1}^G \pi_j \exp \left\{ \tilde{F} \left(\mathbf{w}_i, \mathbf{m}_{ij}, V_{ij}, \tilde{\boldsymbol{\mu}}_j, \tilde{\boldsymbol{\Sigma}}_j, \xi_i \right) \right\}}.$$

Step 2: Update $\hat{\xi}_i, \hat{\mathbf{m}}_{ig}, \hat{V}_{ig}$:

- update $\hat{\xi}_i$ according to Equation 6;
- update $\hat{\mathbf{m}}_{ig}$ by performing one step of Newton's method for approximating the root to the derivative in Equation 7, then let $\hat{m}_{ig(K+1)} = 0$;
- for $k = 1, \dots, K$, update \hat{v}_{igk}^2 by performing one step of Newton's method searching root to the derivative in Equation 8, let $\hat{v}_{ig(K+1)}^2 = 0$, then $\hat{V}_{ig} = \text{diag}(\hat{v}_{ig1}^2, \dots, \hat{v}_{ig(K+1)}^2)$.

Step 3: Update $\tilde{\boldsymbol{\mu}}_g$ and $\tilde{\boldsymbol{\Sigma}}_g$ as

$$\begin{aligned} \hat{\tilde{\boldsymbol{\mu}}}_g &= \frac{\sum_{i=1}^n \hat{z}_{ig} \hat{\mathbf{m}}_{ig}}{\sum_{i=1}^n \hat{z}_{ig}}, \\ \hat{\tilde{\boldsymbol{\Sigma}}}_g &= \frac{\sum_{i=1}^n \hat{z}_{ig} \left[\hat{V}_{ig} + (\hat{\mathbf{m}}_{ig} - \hat{\tilde{\boldsymbol{\mu}}}_g)(\hat{\mathbf{m}}_{ig} - \hat{\tilde{\boldsymbol{\mu}}}_g)^\top \right]}{\sum_{i=1}^n \hat{z}_{ig}}. \end{aligned}$$

Note that the original parameters $\boldsymbol{\mu}_g$ and $\boldsymbol{\Sigma}_g$ can be obtained by the transformation

$$\hat{\boldsymbol{\mu}}_g = B^\top \hat{\boldsymbol{\mu}}_g; \quad \hat{\boldsymbol{\Sigma}}_g = B^\top \hat{\boldsymbol{\Sigma}}_g B.$$

An Aitken acceleration criterion (Aitken, 1926) is employed to stop the iterations. More specifically, at t^{th} iteration, when $t > 2$, calculate

$$a^{(t-1)} = \frac{\ell^{(t)} - \ell^{(m-1)}}{\ell^{(t-1)} - \ell^{(t-2)}},$$

$$\ell_\infty^{(t)} = \ell^{(t-1)} + \frac{1}{1 - a^{(t-1)}} (\ell^{(t)} - \ell^{(t-2)}),$$

where $\ell^{(t)} = \tilde{F}(\mathbf{w}_i, \mathbf{m}_{ig}, V_{ig}, \tilde{\boldsymbol{\mu}}_g, \tilde{\boldsymbol{\Sigma}}_g, \xi_i)$ is the variational Gaussian lower bound who approximates the log likelihood at t^{th} iteration. Then, the algorithm will be stopped when $|\ell_\infty^{(t)} - \ell_\infty^{(t-1)}| < \epsilon$ for a given ϵ (Böhning et al., 1994). In our analysis, we ϵ is set to be 1×10^{-3} .

2.4.1 Initialization

For initialization of \hat{z}_{ig} , we used k -means clustering (MacQueen, 1967; Hartigan and Wong, 1979) on the estimate of the underlying latent variable η_i obtained by first calculating the underlying composition using $\mathbf{w}_i / \sum_{k=1}^{K+1} \mathbf{w}_{ik}$ for each observation; mapping this composition to the latent variable \mathbf{y}_i using the additive log-ratio transformation in Equation 1, and transforming the variable to get $\boldsymbol{\eta}_i$ through Equation 2. For initializing the variational parameters for each observation \mathbf{w}_i , we obtain $\boldsymbol{\eta}_i$ first, same as in the \hat{z}_{ig} initialization step. We use this calculated latent variable $\boldsymbol{\eta}_i$ as initialization of \mathbf{m}_{ig} . V_{ig} for each i are initialized as $K + 1$ diagonal matrix such that $\tilde{V}_{kk} = 1$ for $k = 1, \dots, K$ and $V_{kk} = 0$ for $k = K + 1$. ξ_i 's are initialized using 1. According to the initialization on the group label \hat{z}_{ig} , $\tilde{\boldsymbol{\mu}}_g$ and $\tilde{\boldsymbol{\Sigma}}_g$

are initialized as group-specific mean and covariance of $\boldsymbol{\eta}_i$, respectively.

2.5 Model Selection and Performance Assessment

In the clustering context, the number of components G is unknown. Hence, one typically fits models for a large range of possible G and the number of clusters is then chosen *a posteriori* using a model selection criteria. The Bayesian information criterion (BIC; Schwarz, 1978) is one of the most popular criteria in the model-based clustering literature (McNicholas, 2016).

$$\text{BIC} \approx -2\tilde{\mathcal{L}} + d \log(n),$$

where $\tilde{\mathcal{L}}$, defined in Equation 9, is the variational Gaussian lower bound of the complete data log likelihood, and d is the number of free parameters in the model. Specifically, when fitting a G -component model, $d = \frac{(K+1)K}{2} \times G + K \times G + G - 1$.

When the true class labels are known (e.g., in simulation studies), we assess the performance of our proposed model using the adjusted Rand index (ARI; Hubert and Arabie, 1985). It is a measure of the pairwise agreement between the predicted and true classifications such that an ARI of 1 indicates perfect classification and 0 indicates that the classification obtained is no better than by chance.

3 Simulation Studies and Real Data Analysis

To illustrate the performance of our proposed clustering framework, we conducted two sets of simulation studies. For both studies, the i -th observed counts data \mathbf{W}_i are generated as:

1. First, we generate the total counts $\sum_{k=1}^{K+1} W_{ik}$ as a random number from a uniform distribution $U[5000, 10000]$.

2. Given pre-specified group specific parameters $\boldsymbol{\mu}_g$ and $\boldsymbol{\Sigma}_g$, we transform using Equation 3 to get $\tilde{\boldsymbol{\mu}}_g$ and $\tilde{\boldsymbol{\Sigma}}_g$ and generate $\boldsymbol{\eta}_i$ from $N(\tilde{\boldsymbol{\mu}}_g, \tilde{\boldsymbol{\Sigma}}_g)$.
3. Based on $\boldsymbol{\eta}_i$, we calculate $\boldsymbol{\Theta}_i$ using the inverse additive log-ratio transformation ϕ^{-1} using Equation 4.
4. Using $\boldsymbol{\Theta}_i$ as the underlying composition, together with the total counts generated at the first step, we generate discrete random numbers \mathbf{W}_i from multinomial distributions.
5. To initialize the variational parameters, we need to use the additive log-ratio transformation which takes the log transformation of the observed count for taxa k divided by total count for all taxa for sample i . If there are any 0 in the generated count data, we substitute the 0 with 1 for initialization.

We also compared the performance of our proposed model to a Dirichlet mixture model (Holmes et al., 2012) which is widely used to cluster microbiome data. Implementation of the Dirichlet mixture model is available in the R package `DirichletMultinomial` (Morgan, 2020).

3.1 Simulation Study 1

In this simulation study, we generated 100 datasets where the underlying latent variable \mathbf{Y} came from two component, three-dimensional multivariate Gaussian distributions with mixing proportions $\boldsymbol{\pi} = (0.6, 0.4)$; see Figure 1 (left panel). The first component consists of $n_1 = 600$ observations and the second component consists of $n_2 = 400$ observations. The parameters used to generate the datasets are summarized in Table 1. We fitted the models with $G = 1, \dots, 5$ on all 100 datasets. In 100 out of 100 datasets, BIC selected a two-component model. The models selected by BIC yielded an average ARI = 0.94 with

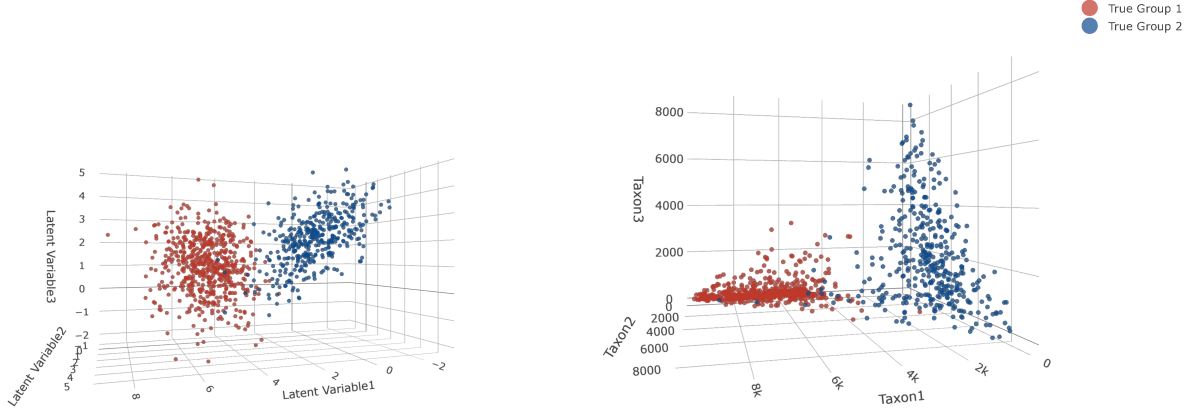


Figure 1: Three dimensional scatter plot of one of the 100 datasets in Simulation Study 1 highlighting the true labels for the latent variable (left) and the first three columns of the count data (right).

standard deviation 0.02. The average and standard deviation of the estimated parameters for the all 100 datasets are summarized in Table 1. Figure 2 illustrates a clear difference in the distribution of the relative abundance of taxa in the two predicted groups. We also ran the Dirichlet-multinomial mixture model for $G = 1 : 4$ and selected the best model using BIC. In all 100 out of 100 datasets, it selected a $G = 4$ model with an average ARI of 0.52 (sd of 0.04). The Dirichlet-multinomial model overestimates the number of components by splitting the true clusters into multiple clusters with some misclassifications among them.

3.2 Simulation Study 2

In this simulation study, we generated 100 datasets with the underlying latent variable \mathbf{Y} from three component five-dimensional multivariate Gaussian distributions (see Figure 3 for the pairwise scatterplot of the underlying latent variable \mathbf{Y}_i).

There are $n_1 = 300$ observations in Group 1, $n_2 = 400$ observations in Group 2, and $n_3 = 200$ observations in Group 3. The true parameters are summarized in Table 2. Figure 4 (left panel) shows the first three dimensions of the latent variable \mathbf{Y}_i 's and Figure 4 (right panel) shows the first three dimensions of the observed counts \mathbf{W}_i 's. There is a more separation between the groups when visualizing the latent variables as opposed to the observed counts.

The proposed algorithm was applied on all 100 datasets where for each dataset, we fitted the models with for $G = 1, \dots, 4$. In 94 out of the 100 datasets, a $G = 3$ model was selected using the BIC, a $G = 2$ was selected for 3 out of the 100 datasets, and $G = 4$ models were selected for the remaining 3 datasets. The overall mean ARI for all 100 datasets was 0.93 (sd of 0.06) and the mean ARI for 94 datasets where a three component model was selected was 0.94 (sd of 0.01). The average and standard deviation of the estimated parameters from the 94 out of the 100 datasets where a three component model was selected are summarized in Table 2. Figure 5 illustrates a clear difference in the distribution of the relative abundance of taxa in the predicted groups. We also ran the Dirichlet-multinomial mixture model for $G = 1 : 4$ and selected the best model using BIC. In all 100 out of 100 datasets, it selected a $G = 4$ model with an average ARI of 0.33 (sd of 0.03).

3.3 Real Data Analysis

We applied our proposed algorithms to three microbiome datasets from two studies:

3.3.1 The Ferretti 2018 Dataset

We applied our algorithm to the Ferretti 2018 dataset (Ferretti et al., 2018) available through the R package `curatedMetagenomicData` (Pasolli et al., 2017) as `FerrettiP_2018` dataset. The study aims to understand the acquisition and development of the infant microbiome and assessed the impact of the maternal microbiomes on the development of infant oral and fecal microbial communities from birth to 4 months of life. Twenty five mother infant pairs who vaginally delivered healthy newborns at full term were recruited for the study. For each mother, stool (proxy for gut microbiome), dorsum tongue swabs (for oral microbiome), vaginal introitus swabs (for vaginal microbiome), intermammary cleft swabs (skin microbiome) and breast milk were obtained. As the DNA extraction from breast milk was not feasible in most cases, they were not analyzed further. All infants were exclusively breastfed at 3 days, 96% at 1 month, and 56% at 4 months and for each newborn, oral cavity and gut samples were taken from birth to up to 4 months. The samples were sequenced using high-resolution shotgun metagenomics (Quince et al., 2017) with an improved strain-level computational profiling of known and poorly characterized microbiome members (Segata, 2018). See Ferretti et al. (2018) for further details. Here, we applied our algorithms to two subsets of the datasets: comparing gut microbiome of the infant with their mothers and comparing oral microbiome of the infants with their mothers.

Gut microbiome subset: This subset of Ferretti 2018 dataset available through R package `curatedMetagenomicData` comprised of 119 samples (23 adults and 96 newborns). As mentioned in Ferretti et al (2018), stool samples of newborns were taken at five different time points: Day 1, Day 3, Day 7, 1 Month and 4 Months. As repeated measurements at different time points are taken on the same individuals and our model currently cannot model that (violates the independence assumption), we only focus on one time point (i.e., Day 1) for the newborns. Hence, the resulting dataset comprises of 42 individuals (23 adults and 19

infants). Here, we focused our analysis on the OTU counts at the genus level data. The heat map of the relative abundance of the top twenty most abundant genera in Figure 6 shows that there are clear differences in the relative abundance of some genera in infants and adults, and therefore suggesting a cluster analysis may be useful. Note that genus **Unknown** is not considered in the heat map.

We utilize the R package **ALDEx2** (Fernandes et al., 2013; Gloor, 2015) for differential abundance analysis to the observed genus counts to identify the genera that are different in adults and infants. This step is analogous to conducting differential expression analysis in RNA-seq studies before performing cluster analysis. As our approach is currently not designed for high dimensional data, we only focus on a small set (top four) of differentially abundant genera and aggregate the remaining genera in a category "Others" to preserve relative abundance. This "Other" genus was then used as the reference level for computing the underlying composition and conducting the additive log-ratio transformation. Here, the genera *Bacteroides*, *Alistipes*, *Subdoligranulum* and *Parabacteroides* are identified as top 4 most differentially abundant genera. We applied our algorithm to this dataset for $G = 1$ to 4 and BIC selected a two-component model with an ARI of 0.81. We also ran the Dirichlet-multinomial mixture model with the same set of genera for $G = 1$ to 4. A two-component model was selected with an ARI of 0.73. Table 3 shows the classification obtained by proposed model and by Dirichlet-multinomial mixture model.

The relative abundance of the four most abundant genera in two predicted clusters is shown in Figure 7. The relative abundance of all four genera is higher and more variable in adults as compared to the infants.

Oral microbiome subset: This subset of Ferretti 2018 dataset available through R package **curatedMetagenomicData** comprised of 62 samples (23 adults and 39 infants). As mentioned in Ferretti et al (2018), oral samples of infants were taken at two different time points: Day

1 and Day 3. Here, as the Day 3 had measurements for all 23 newborns, we use the Day 3 measurements for the analysis. The resulting dataset consists of 46 individuals (23 adults and 23 infants). Here, we again focused our analysis on the OTU counts at the genus level data. The heat map of the relative abundance of the top twenty most abundant genera in Figure 8 shows that there are differences in the relative abundance of some genera in oral microbiome of the infants and adults, and therefore suggesting a cluster analysis may be useful. Note that genus **Unknown** is not considered in the heat map.

The heat map of the relative abundance of the top twenty most abundant genera in Figure 6 shows that there are some differences in the relative abundance of some genera in infants and adults.

Again, we utilize the R package **ALDEx2** for differential abundance analysis on the observed genus counts to identify the genera that are different in adults and infants and select the top four differentially abundant genera. The remaining genera are aggregated in a category "Others" to preserve relative abundance. This "Other" genus was then used as the reference level. Here, the genera *Prevotella*, *Veillonella*, *Actinomyces*, and *Streptococcus* are identified as top four most differentially abundant genera. We applied our algorithm to this dataset for $G = 1$ to 4 and BIC selected a two-component model with a perfect classification. We also ran the Dirichlet-multinomial mixture model with the same set of genera for $G = 1$ to 4 and a two-component model was also selected with a perfect classification. Table 4 shows the classification obtained by the proposed model and by the Dirichlet-multinomial mixture model.

The relative abundance of the four most abundant genera in two predicted clusters is shown in Figure 9. The relative abundance of genera *Prevotella*, *Veillonella*, and *Actinomyces* is higher in adults compared to infants but the relative abundance of the genus *Streptococcus* is higher in infants. This is not surprising as other studies have also shown that the

Streptococcus is one of the early colonizers in the oral cavity (Mason et al., 2018; Xiao et al., 2020).

3.3.2 The Shi 2015 Data

We also applied our algorithm to the Shi 2015 dataset (Shi et al., 2015) available through the R package `curatedMetagenomicData` (Pasolli et al., 2017) as `Shi_2015` dataset. Periodontitis is a common oral disease that affects about 50% of the American adults and is associated with alterations in the subgingival microbiome of individual tooth sites. The study aimed to identify and predict the disease progression using the compositions of the subgingival microbiome. Samples were collected from 12 healthy individuals with chronic periodontitis from multiples tooth sites per individual, before and after nonsurgical therapy that consisted of scaling and root planing. Only the samples from the tooth sites that were clinically resolved after the therapy were selected for the study resulting in an average of two sites per subject. Although samples were obtained from multiple sites of individuals, Shi et al. (2015) state that individual tooth sites are likely to have independent clinical states and unique microbial communities in subgingival pockets, and therefore, we treated them as independent samples for our analysis. This resulted in a total of 48 samples (24 periodontitis samples and 24 recovered samples). The heat map of the relative abundance of the top twenty most abundant genera in Figure 10 shows that there are differences in the relative abundance of some genera among the two clinical state “periodontitis” and “recovered”. Note that genus `Unknown` is not considered in the heat map.

As done previously, we utilize the R package `ALDEx2` for differential abundance analysis on the observed genus counts to identify the genera and selected the top four of differentially abundant genera. The remaining genera are aggregated in a category “Others” to preserve relative abundance. This “Other” genus was then used as the reference level. Here, the

genera *Tannerella*, *Porphyromonas*, *Treponema* and *Streptococcus* are identified as top four most differentially abundant genera. We applied our algorithm to this dataset for $G = 1$ to 4 and BIC selected a two-component model with an ARI of 0.49. We also ran the Dirichlet-multinomial mixture model for $G = 1$ to 4 and a two-component model was selected with an ARI of 0.43. Table 5 shows the classification obtained by proposed model and by Dirichlet-multinomial mixture model.

The relative abundance of the four most abundant genera in two predicted clusters is shown in Figure 11. The genera *Tannerella*, *Porphyromonas*, and *Treponema* have high relative abundance in individuals with “periodontitis” and *Streptococcus* has high relative abundance in “recovered” individuals.

Shi et al. (2015) also utilized the microbiome profiles to classify the clinical state. They performed a supervised classification using the weighted gene-voting algorithm and leave-one-out cross-validation yielding 33 out of 48 samples as correctly classified into the respective clinical state (correct classification rate of 68.75%) whereas 6 samples were misclassified into the incorrect clinical state and 9 samples were not assigned to any clinical state due to low prediction strength. Note that in supervised classification, the group labels are used to build a predictive model which is then used to make predictions on new or “future” observations. Here, we achieved a correction classification rate of 85.42% (i.e., 41/48 correct classification).

4 Conclusion

A model-based clustering framework for microbiome compositional data is developed using a mixture of logistic normal multinomial models. The novelty of this work is multi-fold. Previous work (Xia et al., 2013) has indicated that the logistic normal multinomial models can model the dependency of the bacterial composition in a microbiome compositional data

in a more flexible way than the commonly used Dirichlet-multinomial models. The latent variables in the logistic normal multinomial model are assumed to follow a multivariate Gaussian distribution and a closed form expression of the log-likelihood or posterior distributions of the latent variables do not exist. Hence, prior work on model fitting relied on Markov chain Monte Carlo (MCMC) sampling techniques that come with heavy computational burden. This is compounded in the clustering context where MCMC sampling needs to be utilized at every iteration of the variant of EM algorithm that is typically utilized for parameter estimation. Here, we employed a variational Gaussian approximation to the posterior distribution of the latent variable and implemented a generalized EM algorithm that does not rely on MCMC sampling thus making it feasible to extend these models for clustering. This also opening up the possibility of efficiently scaling and extending these models a high dimensional setting.

Through simulation studies, we have shown that the proposed algorithm delivers accurate parameter recovery and good clustering performance. The proposed method is also illustrated on three real datasets in Section 3.3 where we demonstrate that the proposed models can recover the underlying cluster (group) structure in the real data. While in this work, we focus on small dimensional data by data aggregation to most differentially abundant genera in real data analysis, mixtures of logistic multinomial models can be extended to high-dimensional data by introducing subspace clustering techniques through the latent variable (McNicholas and Murphy, 2008; McNicholas and Murphy, 2010; Bouveyron and Brunet-Saumard, 2014). This will be the topic of some future work. Additionally, it has been well-established that different environmental or biological covariates can affect the microbiome compositions. Some future work will also focus on developing a mixture of logistic normal multinomial regression models to investigate the relationship of biological/environmental covariates with the microbiome compositions within each clusters.

Table 1: True and estimated parameters along with the standard deviations from the one hundred datasets for the latent variable parameters in Simulation Study 1; average ARI= 0.94 (0.02).

Component 1 ($n = 600$)						
Parameter	True			Average of the estimates (sd)		
μ	[5, 2, 1]			[5.00(0.05), 2.00(0.05), 1.00(0.04)]		
Σ	$\begin{bmatrix} 1 & 0.4 & 0 \\ 0.4 & 1.2 & -0.5 \\ 0 & -0.5 & 1 \end{bmatrix}$			$\begin{bmatrix} 1.01(0.07) & 0.42(0.06) & -0.01(0.05) \\ 0.42(0.06) & 1.21(0.08) & -0.50(0.06) \\ -0.01(0.05) & -0.50(0.06) & 0.98(0.07) \end{bmatrix}$		
Component 2 ($n = 400$)						
Parameter	True			Average of the estimates (sd)		
μ	[1, 3, 2]			[1.01(0.07), 3.00(0.05), 2.00(0.05)]		
Σ	$\begin{bmatrix} 1.4 & 0.2 & -0.65 \\ 0.2 & 1 & 0 \\ -0.65 & 0 & 1 \end{bmatrix}$			$\begin{bmatrix} 1.41(0.12) & 0.20(0.07) & -0.65(0.08) \\ 0.20(0.07) & 1.00(0.08) & -0.01(0.05) \\ -0.65(0.08) & -0.01(0.05) & 0.97(0.08) \end{bmatrix}$		

Data Availability Statement: The datasets used in this manuscript are publicly available from the R package `curatedMetagenomicData`.

Table 2: True and Estimated Values for the Latent Variable Parameters in Simulation Study 2; Average ARI= 0.94(0.01).

Component 1 ($n = 300$)										
Parameter	True					Estimated (sd)				
μ	[5, 2, 1, 2, 3]					[5.01(0.09), 2.01(0.06), 1.00(0.08), 2.00(0.07), 3.01(0.06)]				
Σ	$\begin{bmatrix} 2 & -0.2 & 0.8 & -1 & 0 \\ -0.2 & 1 & -0.2 & 0 & -0.4 \\ 0.8 & -0.2 & 1.4 & 0.6 & 0 \\ -1 & 0 & 0.6 & 1.6 & 0.2 \\ 0 & -0.4 & 0 & 0.2 & 1.2 \end{bmatrix}$					$\begin{bmatrix} 2.03(0.17) & -0.17(0.08) & 0.82(0.13) & -0.99(0.11) & 0.02(0.10) \\ -0.17(0.08) & 0.98(0.08) & -0.18(0.07) & -0.01(0.08) & -0.39(0.07) \\ 0.82(0.13) & -0.18(0.07) & 1.42(0.13) & 0.61(0.10) & 0.00(0.08) \\ -0.99(0.11) & -0.01(0.08) & 0.61(0.10) & 1.61(0.14) & 0.19(0.07) \\ 0.02(0.10) & -0.39(0.07) & 0.00(0.08) & 0.19(0.07) & 1.22(0.10) \end{bmatrix}$				
Component 2 ($n = 400$)										
Parameter	True					Estimated (sd)				
μ	[2, 3, 4, 1, 2]					[1.99(0.07), 2.99(0.06), 3.99(0.06), 1.00(0.06), 2.00(0.07)]				
Σ	$\begin{bmatrix} 1.4 & 0.65 & 0.4 & 0 & 0 \\ 0.65 & 1 & 0.2 & 0 & 0.4 \\ 0.4 & 0.2 & 1 & 0.6 & 0 \\ 0 & 0 & 0.6 & 1.2 & 0.8 \\ 0 & 0.4 & 0 & 0.8 & 2 \end{bmatrix}$					$\begin{bmatrix} 1.36(0.11) & 0.62(0.07) & 0.38(0.09) & -0.01(0.08) & -0.01(0.09) \\ 0.62(0.07) & 0.98(0.09) & 0.19(0.07) & -0.01(0.06) & 0.39(0.08) \\ 0.38(0.09) & 0.19(0.07) & 0.99(0.09) & 0.60(0.07) & -0.01(0.08) \\ -0.01(0.08) & -0.01(0.06) & 0.60(0.07) & 1.19(0.08) & 0.78(0.09) \\ -0.01(0.09) & 0.39(0.08) & -0.01(0.08) & 0.78(0.09) & 1.97(0.15) \end{bmatrix}$				
Component 3 ($n = 200$)										
Parameter	True					Estimated (sd)				
μ	[1, 1, 1, 1, 1]					[1.00(0.08), 0.98(0.07), 1.00(0.09), 1.01(0.09), 1.01(0.08)]				
Σ	$\begin{bmatrix} 1 & 0 & 0 & 0 & 0 \\ 0 & 1 & 0 & 0 & 0 \\ 0 & 0 & 1 & 0 & 0 \\ 0 & 0 & 0 & 1 & 0 \\ 0 & 0 & 0 & 0 & 1 \end{bmatrix}$					$\begin{bmatrix} 1.00(0.13) & -0.01(0.08) & -0.02(0.08) & -0.02(0.08) & -0.02(0.07) \\ -0.01(0.08) & 0.97(0.11) & -0.01(0.09) & 0.00(0.08) & 0.00(0.07) \\ -0.02(0.08) & -0.01(0.09) & 0.99(0.12) & -0.01(0.08) & 0.00(0.08) \\ -0.02(0.08) & 0.00(0.08) & -0.01(0.08) & 0.98(0.11) & 0.00(0.07) \\ -0.02(0.07) & 0.00(0.07) & 0.00(0.08) & 0.00(0.07) & 0.98(0.10) \end{bmatrix}$				

Table 3: Cross tabulation of the clusters obtained by our proposed algorithm and Dirichlet-multinomial mixture model on the gut microbiome subset.

Proposed algorithm (ARI: 0.81)		Dirichlet-multinomial mixture model (ARI: 0.73)	
Estimated Clusters		Estimated Clusters	
1	2	1	2
Infant	18	1	2
Adult	1	22	22

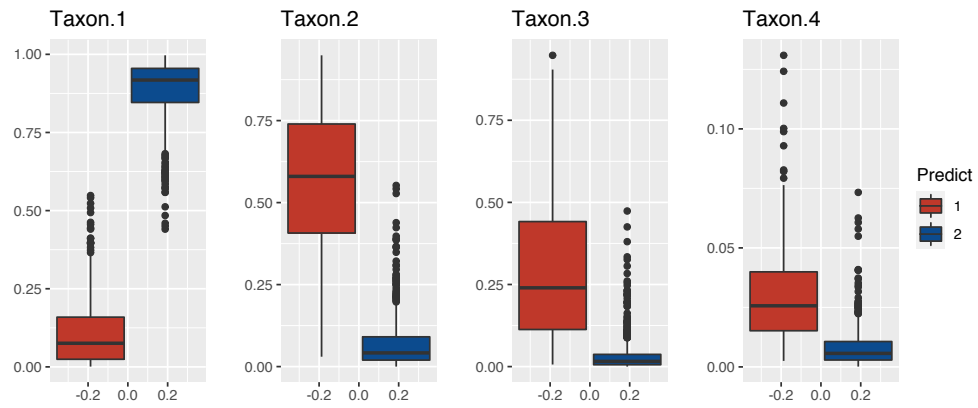


Figure 2: Boxplots of the relative abundance of observed counts of the four taxa for the predicted clusters for one of the 100 datasets in Simulation 1. For this dataset, ARI was 0.95.

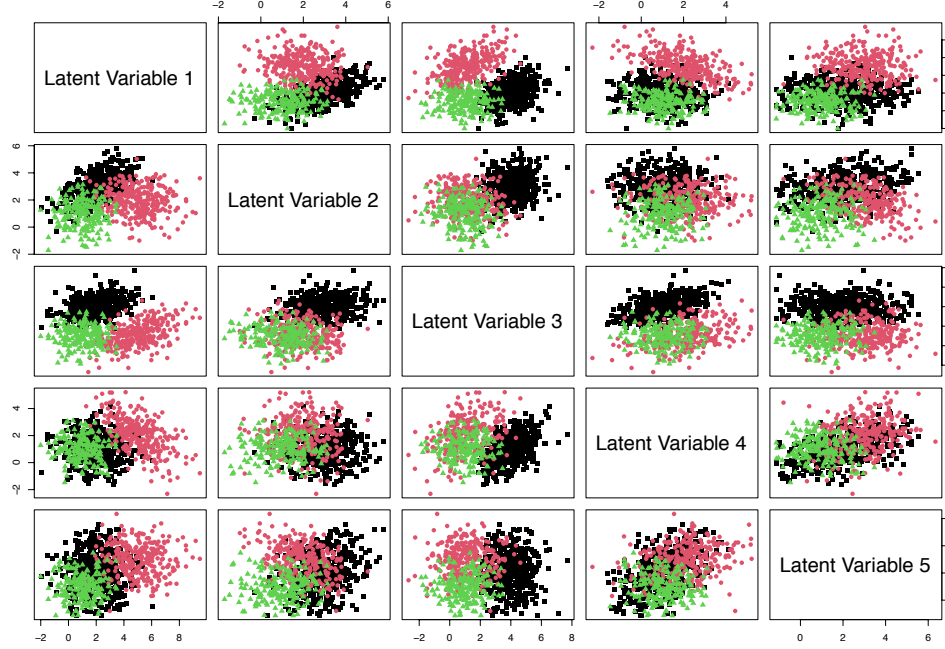


Figure 3: Pairwise scatter plot of one of the 100 datasets in Simulation Study 2 highlighting the true labels for the latent variables. For this dataset, ARI was 0.95.

Table 4: Cross tabulation of the clusters obtained by our proposed algorithm and Dirichlet-multinomial mixture model on the oral microbiome subset.

	Proposed algorithm (ARI: 1)		Dirichlet-multinomial mixture model (ARI: 1)	
	Estimated Clusters		Estimated Clusters	
	1	2	1	2
Infant	23	-	23	-
Adult	-	23	-	23

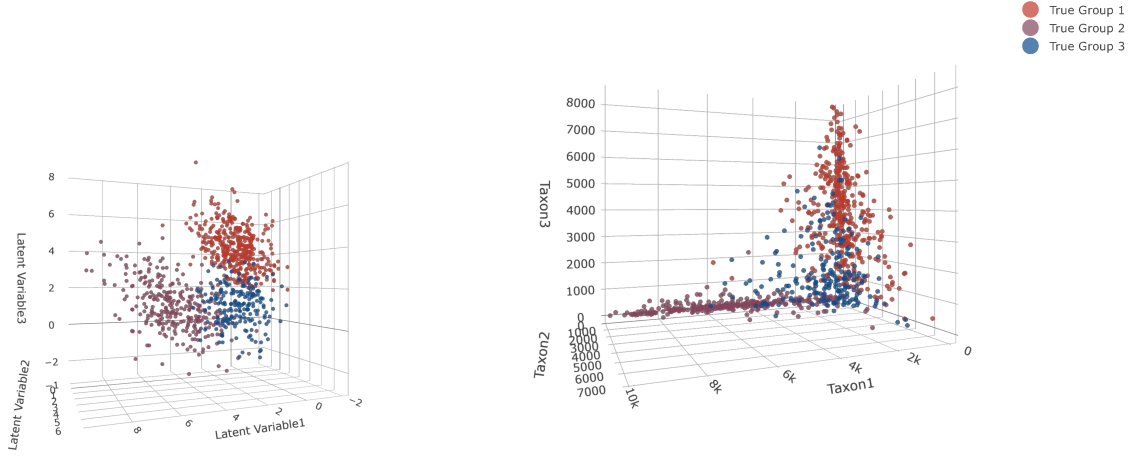


Figure 4: Three dimensional scatter plot of one of the 100 datasets in Simulation Study 2 highlighting the true labels for the latent variable (left) and the first three columns of the count data (right).

Table 5: Cross tabulation of the clusters obtained by our proposed algorithm and Dirichlet-multinomial mixture model on the oral microbiome subset from Shi et al (2015).

	Proposed algorithm (ARI: 0.49)		Dirichlet-multinomial mixture model (ARI: 0.43)	
	Estimated Clusters		Estimated Clusters	
	1	2	1	2
Periodontitis	18	6	18	6
Recovered	1	23	2	22

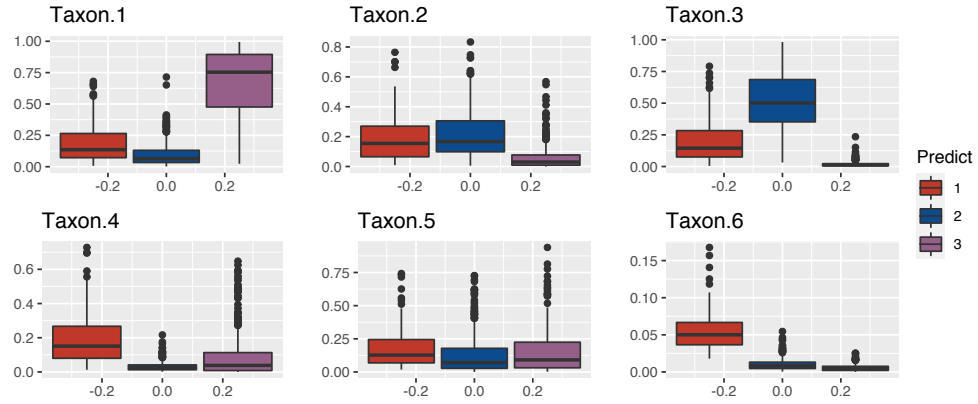


Figure 5: Boxplots of the relative abundance of observed counts of the four taxa for the predicted clusters for one of the 100 datasets in Simulation 4. For this dataset, ARI was 0.95.

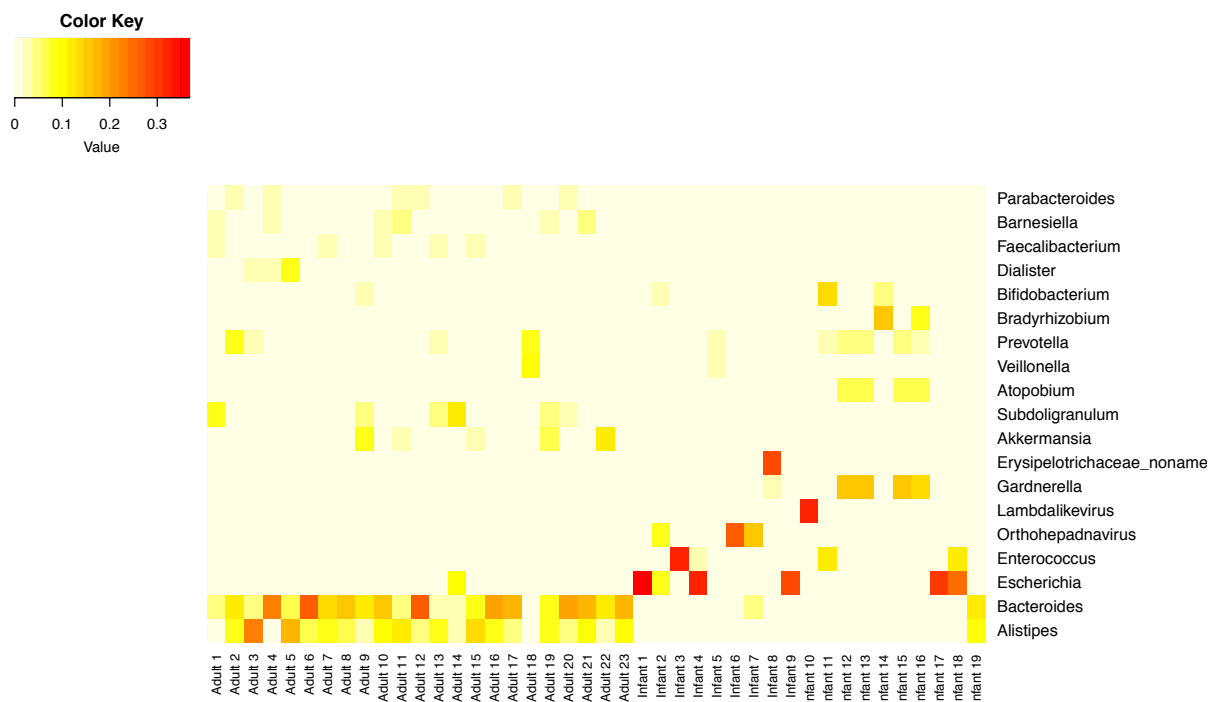


Figure 6: Heat map of the relative abundance of the top twenty most abundant genera for the gut microbiome subset.

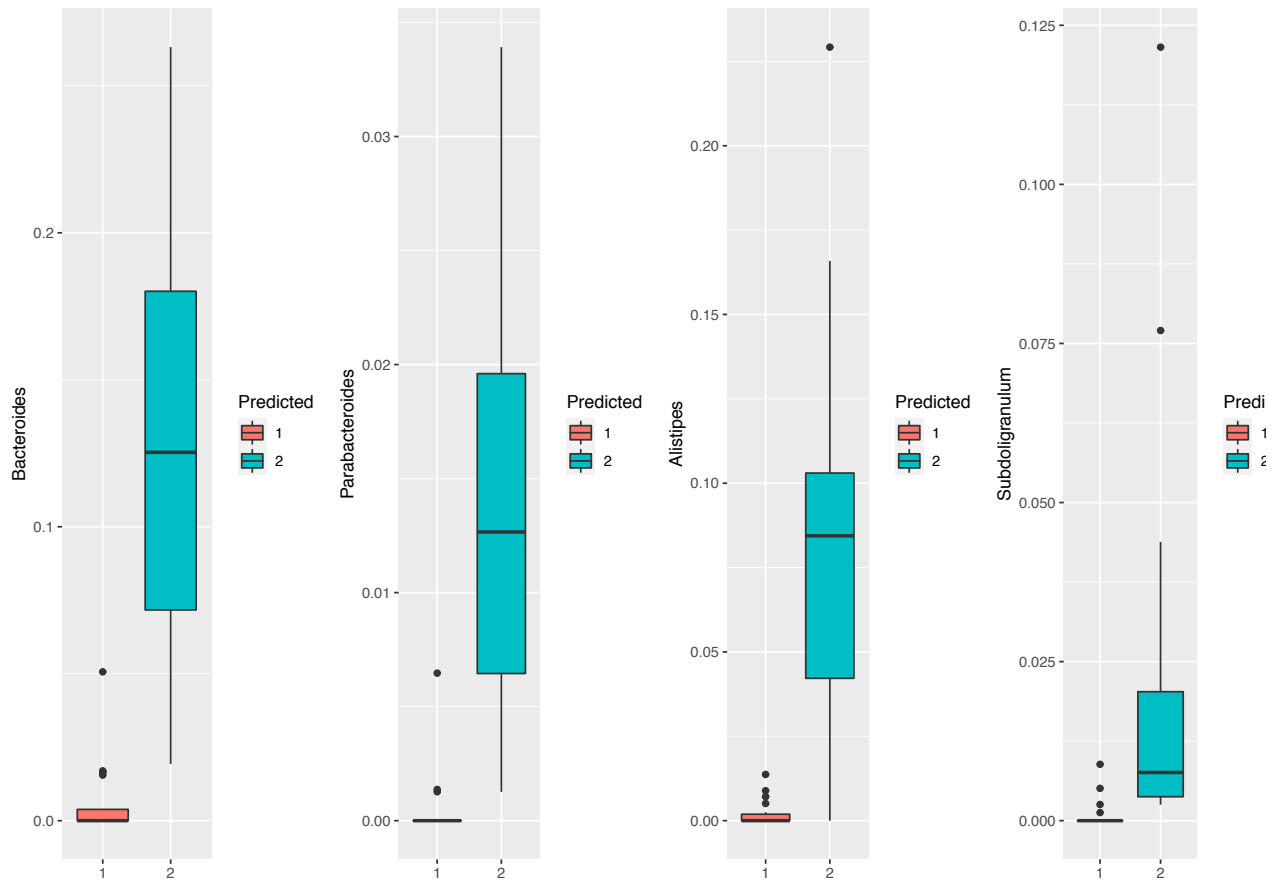


Figure 7: Box plots showing the underlying composition of the four most abundant genera in each of the predicted clusters 1 and 2 on gut microbiome subset from Ferretti 2018.

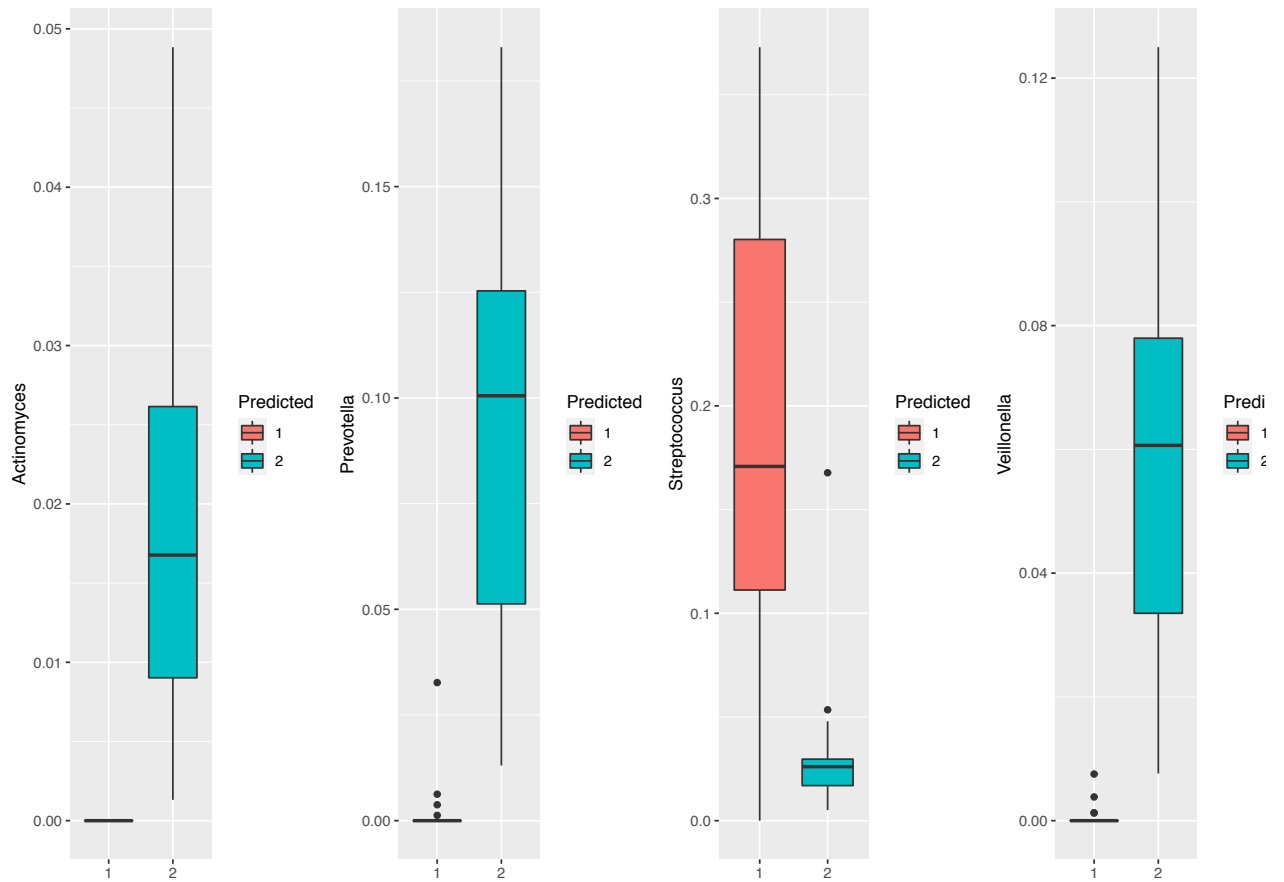


Figure 9: Box plots showing the underlying composition of the four most abundant genera in each of the predicted clusters 1 and 2 on oral microbiome subset from Ferretti 2018.

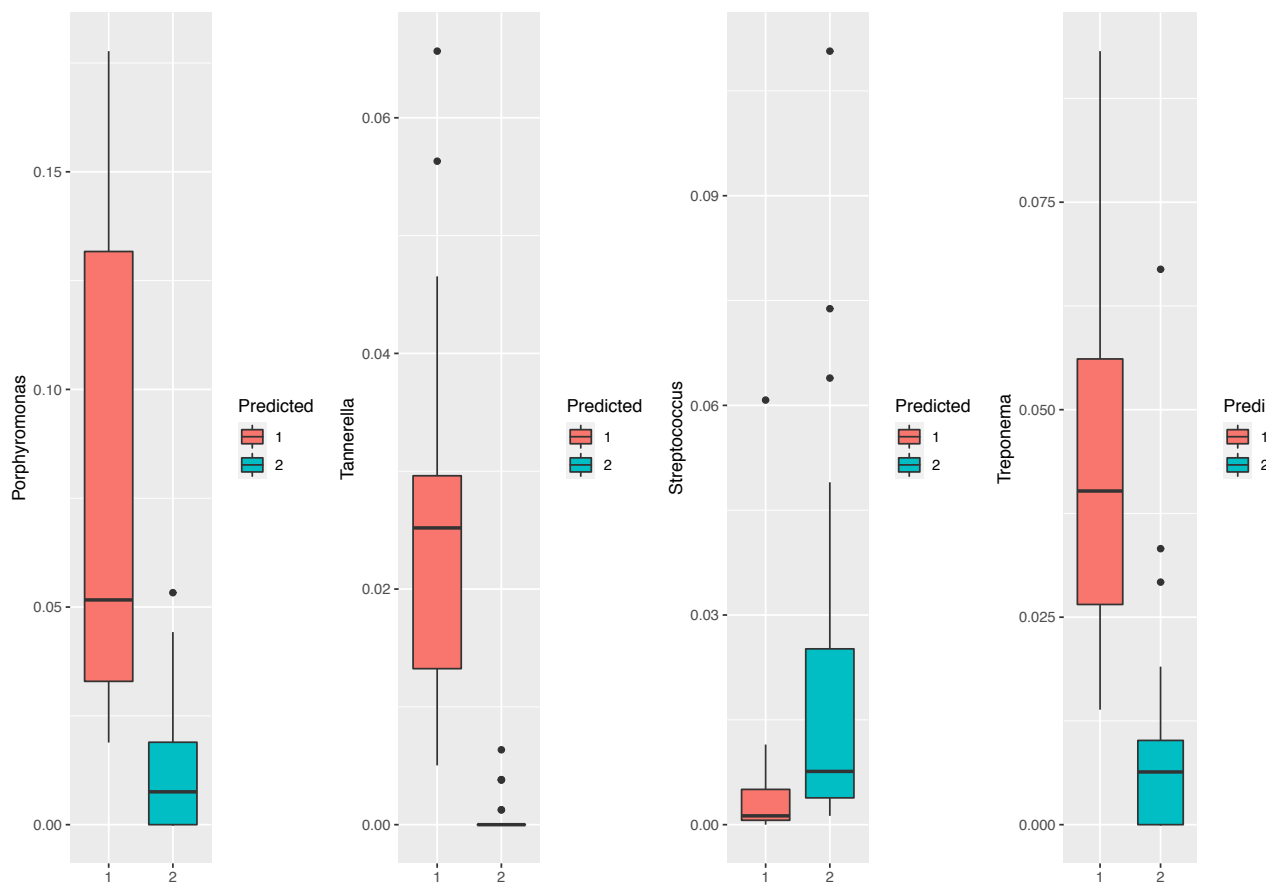


Figure 11: Box plots showing the underlying composition of the four most abundant genera in each of the predicted clusters 1 and 2 on Shi 2015 dataset.

References

- Äijö, T., Müller, C. L., and Bonneau, R. (2018). Temporal probabilistic modeling of bacterial compositions derived from 16s rrna sequencing. *Bioinformatics*, 34(3):372–380.
- Aitchison, J. (1982). The statistical analysis of compositional data. *Journal of the Royal Statistical Society: Series B (Methodological)*, 44(2):139–160.
- Aitken, A. C. (1926). A series formula for the roots of algebraic and transcendental equations. *Proceedings of the Royal Society of Edinburgh*, 45:14–22.
- Archambeau, C., Cornford, D., Opper, M., and Shawe-Taylor, J. (2007). Gaussian process approximations of stochastic differential equations. *Journal of Machine Learning Research*, 1:1–16.
- Arridge, S. R., Ito, K., Jin, B., and Zhang, C. (2018). Variational gaussian approximation for poisson data. *Inverse Problems*, 34(2):025005.
- Barber, D. and Bishop, C. M. (1998). Ensemble learning in bayesian neural networks. *Nato ASI Series F Computer and Systems Sciences*, 168:215–238.
- Bishop, C. M. (2006). *Pattern recognition and machine learning*. springer.
- Blei, D. and Lafferty, J. (2006). Correlated topic models. *Advances in Neural Information Processing Systems*, 18:147.
- Blei, D. M., Kucukelbir, A., and McAuliffe, J. D. (2017). Variational inference: A review for statisticians. *Journal of the American Statistical Association*, 112(518):859–877.
- Böhning, D., Dietz, E., Schaub, R., Schlattmann, P., and Lindsay, B. G. (1994). The distri-

- bution of the likelihood ratio for mixtures of densities from the one-parameter exponential family. *Annals of the Institute of Statistical Mathematics*, 46(2):373–388.
- Bouveyron, C. and Brunet-Saumard, C. (2014). Model-based clustering of high-dimensional data: A review. *Computational Statistics & Data Analysis*, 71:52–78.
- Cao, Y., Zhang, A., and Li, H. (2017). Multi-sample estimation of bacterial composition matrix in metagenomics data. *arXiv preprint arXiv:1706.02380*.
- Caporaso, J. G., Lauber, C. L., Costello, E. K., Berg-Lyons, D., Gonzalez, A., Stombaugh, J., Knights, D., Gajer, P., Ravel, J., Fierer, N., et al. (2011). Moving pictures of the human microbiome. *Genome Biology*, 12(5):R50.
- Challis, E. and Barber, D. (2013). Gaussian kullback-leibler approximate inference. *The Journal of Machine Learning Research*, 14(1):2239–2286.
- Chen, J. and Li, H. (2013). Variable selection for sparse dirichlet-multinomial regression with an application to microbiome data analysis. *The Annals of Applied Statistics*, 7(1).
- Dempster, A. P., Laird, N. M., and Rubin, D. B. (1977). Maximum likelihood from incomplete data via the em algorithm. *Journal of the Royal Statistical Society: Series B (Methodological)*, 39(1):1–22.
- Eckburg, P. B., Bik, E. M., Bernstein, C. N., Purdom, E., Dethlefsen, L., Sargent, M., Gill, S. R., Nelson, K. E., and Relman, D. A. (2005). Diversity of the human intestinal microbial flora. *science*, 308(5728):1635–1638.
- Fernandes, A., Macklaim, J., Linn, T., Reid, G., and Gloor, G. (2013). Anova-like differential gene expression analysis of single-organism and meta-rna-seq. *PLoS One*, 8(7):e67019.

- Ferretti, P., Pasolli, E., Tett, A., Asnicar, F., Gorfer, V., Fedi, S., Armanini, F., Truong, D. T., Manara, S., Zolfo, M., et al. (2018). Mother-to-infant microbial transmission from different body sites shapes the developing infant gut microbiome. *Cell Host & Microbe*, 24(1):133–145.
- Fraher, M. H., O’toole, P. W., and Quigley, E. M. (2012). Techniques used to characterize the gut microbiota: a guide for the clinician. *Nature Reviews Gastroenterology & hepatology*, 9(6):312.
- Frühwirth-Schnatter, S. (2006). *Finite mixture and Markov switching models*. Springer Science & Business Media.
- Gloor, G. (2015). Aldex2: Anova-like differential expression tool for compositional data. *ALDEX manual modular*, 20:1–11.
- Greenblum, S., Turnbaugh, P. J., and Borenstein, E. (2012). Metagenomic systems biology of the human gut microbiome reveals topological shifts associated with obesity and inflammatory bowel disease. *Proceedings of the National Academy of Sciences*, 109(2):594–599.
- Hamady, M. and Knight, R. (2009). Microbial community profiling for human microbiome projects: Tools, techniques, and challenges. *Genome Research*, 19(7):1141–1152.
- Hartigan, J. A. and Wong, M. A. (1979). A k-means clustering algorithm. *Applied Statistics*, 28(1):100–108.
- Holmes, I., Harris, K., and Quince, C. (2012). Dirichlet multinomial mixtures: generative models for microbial metagenomics. *PLOS One*, 7(2).
- Hubert, L. and Arabie, P. (1985). Comparing partitions. *Journal of classification*, 2(1):193–218.

- Joseph, N., Paulson, C., Corrada Bravo, H., and Pop, M. (2013). Robust methods for differential abundance analysis in marker gene surveys. *Nature Methods*, 10:1200–1202.
- Khan, E., Mohamed, S., and Murphy, K. P. (2012). Fast bayesian inference for non-conjugate gaussian process regression. In *Advances in Neural Information Processing Systems*, pages 3140–3148.
- Koeth, R. A., Wang, Z., Levison, B. S., Buffa, J. A., Org, E., Sheehy, B. T., Britt, E. B., Fu, X., Wu, Y., Li, L., et al. (2013). Intestinal microbiota metabolism of l-carnitine, a nutrient in red meat, promotes atherosclerosis. *Nature Medicine*, 19(5):576.
- Kuczynski, J., Lauber, C. L., Walters, W. A., Parfrey, L. W., Clemente, J. C., Gevers, D., and Knight, R. (2012). Experimental and analytical tools for studying the human microbiome. *Nature Reviews Genetics*, 13(1):47–58.
- Ley, R. E., Peterson, D. A., and Gordon, J. I. (2006). Ecological and evolutionary forces shaping microbial diversity in the human intestine. *Cell*, 124(4):837–848.
- Li, H. (2015). Microbiome, metagenomics, and high-dimensional compositional data analysis. *Annual Review of Statistics and Its Application*, 2:73–94.
- MacQueen, J. B. (1967). *Some methods for classification and analysis of multivariate observations*. In *Proceedings of the Fifth Berkeley Symposium on Mathematical Statistics and Probability*. University of California Press, Berkeley, CA.
- Mason, M. R., Chambers, S., Dabdoub, S. M., Thikkurissy, S., and Kumar, P. S. (2018). Characterizing oral microbial communities across dentition states and colonization niches. *Microbiome*, 6(1):67.

- McLachlan, G. and Peel, D. (2000). *Wiley series in probability and statistics*. John Wiley & Sons Hoboken, NJ.
- McNicholas, P. D. (2016). *Mixture model-based classification*. Chapman and Hall/CRC.
- McNicholas, P. D. and Murphy, T. B. (2008). Parsimonious gaussian mixture models. *Statistics and Computing*, 18(3):285–296.
- McNicholas, P. D. and Murphy, T. B. (2010). Model-based clustering of microarray expression data via latent gaussian mixture models. *Bioinformatics*, 26(21):2705–2712.
- Morgan, M. (2020). *DirichletMultinomial: Dirichlet-Multinomial Mixture Model Machine Learning for Microbiome Data*. R package version 1.32.0.
- Morgan, X. C. and Huttenhower, C. (2012). Human microbiome analysis. *PLOS Computational Biology*, 8(12):e1002808.
- Papastamoulis, P., Martin-Magniette, M.-L., and Maugis-Rabusseau, C. (2016). On the estimation of mixtures of poisson regression models with large number of components. *Computational Statistics & Data Analysis*, 93:97–106.
- Pasolli, E., Schiffer, L., Manghi, P., Renson, A., Obenchain, V., Truong, D. T., Beghini, F., Malik, F., Ramos, M., Dowd, J. B., Huttenhower, C., Morgan, M., Segata, N., and Waldron, L. (2017). Accessible, curated metagenomic data through experimenthub. *Nature Methods*, 14(11):1023–1024.
- Qin, J., Li, Y., Cai, Z., Li, S., Zhu, J., Zhang, F., Liang, S., Zhang, W., Guan, Y., Shen, D., et al. (2012). A metagenome-wide association study of gut microbiota in type 2 diabetes. *Nature*, 490(7418):55–60.

- Quince, C., Walker, A. W., Simpson, J. T., Loman, N. J., and Segata, N. (2017). Shotgun metagenomics, from sampling to analysis. *Nature Biotechnology*, 35(9):833–844.
- Rau, A., Celeux, G., Martin-Magniette, M.-L., and Maugis-Rabusseau, C. (2011). Clustering high-throughput sequencing data with poisson mixture models. Technical report, INRIA, Saclay, Ile-de-France.
- Schwarz, G. (1978). Estimating the dimension of a model. *The Annals of Statistics*, 6(2):461–464.
- Segata, N. (2018). On the road to strain-resolved comparative metagenomics. *mSystems*, 3(2):e00190–17.
- Shi, B., Chang, M., Martin, J., Mitreva, M., Lux, R., Klokkevold, P., Sodergren, E., Weinstein, G. M., Haake, S. K., and Li, H. (2015). Dynamic changes in the subgingival microbiome and their potential for diagnosis and prognosis of periodontitis. *MBio*, 6(1):e01926–14.
- Si, Y., Liu, P., Li, P., and Brutnell, T. P. (2014). Model-based clustering for rna-seq data. *Bioinformatics*, 30(2):197–205.
- Silva, A., Rothstein, S. J., McNicholas, P. D., and Subedi, S. (2019). A multivariate poisson-log normal mixture model for clustering transcriptome sequencing data. *BMC Bioinformatics*, 20(1):394.
- Silverman, J. D., Durand, H. K., Bloom, R. J., Mukherjee, S., and David, L. A. (2018). Dynamic linear models guide design and analysis of microbiota studies within artificial human guts. *Microbiome*, 6(1):1–20.

- Streit, W. R. and Schmitz, R. A. (2004). Metagenomics—the key to the uncultured microbes. *Current Opinion in Microbiology*, 7(5):492–498.
- Subedi, S., Neish, D., Bak, S., and Feng, Z. (2020). Cluster analysis of microbiome data by using mixtures of Dirichlet-multinomial regression models. *Journal of Royal Statistical Society. Series C*, 69(5):1163–1187.
- Turnbaugh, P. J., Hamady, M., Yatsunenko, T., Cantarel, B. L., Duncan, A., Ley, R. E., Sogin, M. L., Jones, W. J., Roe, B. A., Affourtit, J. P., et al. (2009). A core gut microbiome in obese and lean twins. *nature*, 457(7228):480–484.
- Wadsworth, W. D., Argiento, R., Guindani, M., Galloway-Pena, J., Shelburne, S. A., and Vannucci, M. (2017). An integrative bayesian dirichlet-multinomial regression model for the analysis of taxonomic abundances in microbiome data. *BMC Bioinformatics*, 18(1):94.
- Wainwright, M. J., Jordan, M. I., et al. (2008). Graphical models, exponential families, and variational inference. *Foundations and Trends® in Machine Learning*, 1(1–2):1–305.
- Xia, F., Chen, J., Fung, W. K., and Li, H. (2013). A logistic normal multinomial regression model for microbiome compositional data analysis. *Biometrics*, 69(4):1053–1063.
- Xiao, J., Fiscella, K. A., and Gill, S. R. (2020). Oral microbiome: possible harbinger for children’s health. *International Journal of Oral Science*, 12(1):1–13.
- Xu, L., Paterson, A. D., Turpin, W., and Xu, W. (2015). Assessment and selection of competing models for zero-inflated microbiome data. *PLOS One*, 10(7).
- Xu, T., Demmer, R. T., and Li, G. (2020). Zero-inflated poisson factor model with application to microbiome read counts. *Biometrics*.

- Yatsunenko, T., Rey, F. E., Manary, M. J., Trehan, I., Dominguez-Bello, M. G., Contreras, M., Magris, M., Hidalgo, G., Baldassano, R. N., Anokhin, A. P., et al. (2012). Human gut microbiome viewed across age and geography. *Nature*, 486(7402):222–227.
- Zhang, X., Mallick, H., Tang, Z., Zhang, L., Cui, X., Benson, A. K., and Yi, N. (2017). Negative binomial mixed models for analyzing microbiome count data. *BMC Bioinformatics*, 18(1):4.
- Zhang, X. and Yi, N. (2020). Fast zero-inflated negative binomial mixed modeling approach for analyzing longitudinal metagenomics data. *Bioinformatics*, 36(8):2345–2351.
- Zhong, S. and Ghosh, J. (2003). A unified framework for model-based clustering. *Journal of Machine Learning Research*, 4(Nov):1001–1037.

A Mathematical Detail

Consider the following transformed parameter $\boldsymbol{\eta}$ from \mathbf{Y} :

$$\boldsymbol{\eta} = B\mathbf{Y}, \quad \text{where } B = \begin{pmatrix} 1 & 0 & \dots & 0 \\ 0 & 1 & \dots & 0 \\ \vdots & \vdots & \dots & \vdots \\ 0 & 0 & \dots & 1 \\ 0 & 0 & \dots & 0 \end{pmatrix},$$

is a $(K + 1) \times K$ matrix which takes the form as an identity matrix attached by a row of K zeros. Given the assumption that the true distribution of \mathbf{Y} is $N(\boldsymbol{\mu}, \boldsymbol{\Sigma})$, we have the true

distribution of $\boldsymbol{\eta}$ to be Gaussian too, with mean $\tilde{\boldsymbol{\mu}}$ and covariance matrix $\tilde{\boldsymbol{\Sigma}}$, where

$$\tilde{\boldsymbol{\mu}} = B\boldsymbol{\mu} = (\boldsymbol{\mu}, 0)^\top; \tilde{\boldsymbol{\Sigma}} = B\boldsymbol{\Sigma}B^\top = \left(\begin{array}{c|c} \boldsymbol{\Sigma} & \mathbf{0}_{K \times 1} \\ \hline \mathbf{0}_{1 \times K} & 0 \end{array} \right).$$

For computational convenience, we further assume that V has a diagonal structure, with each diagonal element denoted as v_k^2 such that

$$v_k^2 = \begin{cases} v_k^2, & k = 1, \dots, K \\ 0, & k = K + 1. \end{cases}$$

We also denote the k -th element of \mathbf{m} as m_k such that

$$m_k = \begin{cases} m_k, & k = 1, \dots, K \\ 0, & k = K + 1. \end{cases}$$

Recall that we have the following decomposition of the ELBO

$$F(q(\boldsymbol{\eta}), \mathbf{w}) = F(\mathbf{m}, V) = - \int q(\boldsymbol{\eta}) \log q(\boldsymbol{\eta}) d\boldsymbol{\eta} + \int q(\boldsymbol{\eta}) \log p(\boldsymbol{\eta}) d\boldsymbol{\eta} + \int q(\boldsymbol{\eta}) \log p(\mathbf{w}|\boldsymbol{\eta}) d\boldsymbol{\eta};$$

among which, the first integral by definition is the entropy of the variational Gaussian distribution $q(\boldsymbol{\eta}|\mathbf{m}, V)$:

$$- \int q(\boldsymbol{\eta}) \log q(\boldsymbol{\eta}) d\boldsymbol{\eta} = -\mathbb{E}_{q(\boldsymbol{\eta}|\mathbf{m}, V)} (q(\boldsymbol{\eta})) = \frac{1}{2} \sum_{k=1}^K \log(v_k^2) + \frac{K}{2} \log(2\pi) + \frac{K}{2}.$$

The second integral can be evaluated explicitly as well, which turn into the expected value

of the log density function of $p(\boldsymbol{\eta}) = \mathcal{N}(\boldsymbol{\eta}|\tilde{\boldsymbol{\mu}}, \tilde{\boldsymbol{\Sigma}})$ with respect to $q(\boldsymbol{\eta}|\mathbf{m}, V)$:

$$\begin{aligned} \int q(\boldsymbol{\eta}) \log p(\boldsymbol{\eta}) d\boldsymbol{\eta} &= \mathbb{E}_{q(\boldsymbol{\eta}|\mathbf{m}, V)} (\log p(\boldsymbol{\eta})) \\ &= \mathbb{E}_{q(\boldsymbol{\eta}|\mathbf{m}, V)} \left(-\frac{K}{2} \log(2\pi) - \frac{1}{2} \log |\tilde{\boldsymbol{\Sigma}}| - \frac{1}{2} (\boldsymbol{\eta} - \boldsymbol{\mu})^\top \tilde{\boldsymbol{\Sigma}}^{-1} (\boldsymbol{\eta} - \boldsymbol{\mu}) \right) \\ &= -\frac{K}{2} \log(2\pi) - \frac{1}{2} \log |\tilde{\boldsymbol{\Sigma}}| - \frac{1}{2} (\mathbf{m} - \tilde{\boldsymbol{\mu}})^\top \tilde{\boldsymbol{\Sigma}}^{-1} (\mathbf{m} - \tilde{\boldsymbol{\mu}}) - \frac{1}{2} \text{Tr}(\tilde{\boldsymbol{\Sigma}}^{-1} V). \end{aligned}$$

Due to the special structure of $\tilde{\boldsymbol{\Sigma}}$, we have $|\tilde{\boldsymbol{\Sigma}}| = 0$ and $\tilde{\boldsymbol{\Sigma}}^{-1}$ does not exist, which brings in a computational issue. Therefore, we substitute $|\tilde{\boldsymbol{\Sigma}}|$ by $|\boldsymbol{\Sigma}| = |B^\top \tilde{\boldsymbol{\Sigma}} B|$ and $\tilde{\boldsymbol{\Sigma}}^{-1}$ by the generalized inverse of $\tilde{\boldsymbol{\Sigma}}$

$$\tilde{\boldsymbol{\Sigma}}^* = \left(\begin{array}{c|c} \boldsymbol{\Sigma}^{-1} & \mathbf{0}_{K \times 1} \\ \hline \mathbf{0}_{1 \times K} & 0 \end{array} \right).$$

Hence we have

$$\begin{aligned} \int q(\boldsymbol{\eta}) \log p(\boldsymbol{\eta}) d\boldsymbol{\eta} &= -\frac{K}{2} \log(2\pi) - \frac{1}{2} \log |\boldsymbol{\Sigma}| - \frac{1}{2} (\mathbf{m} - \tilde{\boldsymbol{\mu}})^\top \tilde{\boldsymbol{\Sigma}}^* (\mathbf{m} - \tilde{\boldsymbol{\mu}}) - \frac{1}{2} \text{Tr}(\tilde{\boldsymbol{\Sigma}}^* V) \\ &= -\frac{K}{2} \log(2\pi) - \frac{1}{2} \log |B^\top \tilde{\boldsymbol{\Sigma}} B| - \frac{1}{2} (\mathbf{m} - \tilde{\boldsymbol{\mu}})^\top \tilde{\boldsymbol{\Sigma}}^* (\mathbf{m} - \tilde{\boldsymbol{\mu}}) - \frac{1}{2} \text{Tr}(\tilde{\boldsymbol{\Sigma}}^* V). \end{aligned}$$

The third integral is intractable, because of the log-sum exponential term. We upper bound this term with a Taylor expansion similar to previous literature (Blei and Lafferty, 2006) resulting in the following

$$\begin{aligned} \mathbb{E}_{q(\boldsymbol{\eta}|\mathbf{m}, V)} \left[\log \left(\sum_{k=1}^{K+1} \exp \eta_k \right) \right] &\leq \xi^{-1} \left\{ \sum_{k=1}^{K+1} \mathbb{E}_{q(\boldsymbol{\eta}|\mathbf{m}, V)} [\exp(\eta_k)] \right\} - 1 + \log(\xi) \\ &= \xi^{-1} \left\{ \sum_{k=1}^{K+1} \exp \left(m_k + \frac{v_k^2}{2} \right) \right\} - 1 + \log(\xi). \end{aligned}$$

Therefore, the third integral is lower bounded by

$$\begin{aligned}
\int q(\boldsymbol{\eta}) \log p(\mathbf{w}|\boldsymbol{\eta}) d\boldsymbol{\eta} &= \mathbb{E}_{q(\boldsymbol{\eta}|\mathbf{m}, V)} \left[\mathbf{w}^\top \boldsymbol{\eta} - \sum_{k=1}^{K+1} w_k \log \left(\sum_{k=1}^{K+1} \exp \eta_k \right) \right] \\
&= \mathbf{w}^\top \mathbf{m} - \left(\sum_{k=1}^{K+1} w_k \right) \mathbb{E}_{q(\boldsymbol{\eta}|\mathbf{m}, V)} \left[\log \left(\sum_{k=1}^{K+1} \exp \eta_k \right) \right] \\
&\geq \mathbf{w}^\top \mathbf{m} - \left(\sum_{k=1}^{K+1} w_k \right) \left\{ \xi^{-1} \left[\sum_{k=1}^{K+1} \exp \left(m_k + \frac{v_k^2}{2} \right) \right] - 1 + \log(\xi) \right\}.
\end{aligned}$$

Combining all three integrals, we obtain a concave variational Gaussian lower bound to the model evidence

$$\begin{aligned}
\tilde{F}(\mathbf{m}, V, \tilde{\boldsymbol{\mu}}, \tilde{\boldsymbol{\Sigma}}, \xi) &= \mathbf{w}^\top \mathbf{m} - \left(\sum_{k=1}^{K+1} w_k \right) \left\{ \xi^{-1} \left[\sum_{k=1}^{K+1} \exp \left(m_k + \frac{v_k^2}{2} \right) \right] - 1 + \log(\xi) \right\} \\
&\quad - \frac{1}{2} \log |B^\top \tilde{\boldsymbol{\Sigma}} B| - \frac{1}{2} (\mathbf{m} - \tilde{\boldsymbol{\mu}})^\top \tilde{\boldsymbol{\Sigma}}^* (\mathbf{m} - \tilde{\boldsymbol{\mu}}) - \frac{1}{2} \text{Tr}(\tilde{\boldsymbol{\Sigma}}^* V) \\
&\quad + \frac{1}{2} \sum_{k=1}^K \log(v_k^2) + \frac{K}{2}.
\end{aligned}$$

We maximize this lower bound with respect to the variational parameters ξ, \mathbf{m}, V .

First, we maximize the lower bound 5 with respect to ξ . The derivative with respect to ξ is

$$\frac{\partial \tilde{F}}{\partial \xi} = \left(\sum_{k=1}^{K+1} w_k \right) \left\{ -\xi^{-2} \left[\sum_{k=1}^{K+1} \exp \left(m_k + \frac{v_k^2}{2} \right) \right] + \xi^{-1} \right\},$$

which yields an optimizer at

$$\hat{\xi} = \sum_{k=1}^{K+1} \exp \left(m_k + \frac{v_k^2}{2} \right).$$

Second, we maximize with respect to \mathbf{m} , of which the derivative is given as

$$\frac{\partial \tilde{F}}{\partial \mathbf{m}} = \mathbf{w} - \tilde{\boldsymbol{\Sigma}}^* (\mathbf{m} - \tilde{\boldsymbol{\mu}}) - \left(\sum_{k=1}^{K+1} \mathbf{w}_k \right) \xi^{-1} \exp \left(\mathbf{m} + \frac{\mathbf{v}^2}{2} \right),$$

with $\mathbf{v}^2 = (v_1^2, \dots, v_K^2, 0)$ denoting the diagonal element of V as a vector. There is no

analytical solution to this derivative and so we use Newton's method to approximate the root to this derivative, with a constrain that the $(K+1)$ -th element is zero. The procedure requires the Hessian matrix with respect to \mathbf{m} :

$$H_{\mathbf{m}} = -\tilde{\Sigma}^* - \left(\sum_{k=1}^{K+1} \mathbf{w}_k \right) \xi^{-1} \text{diag} \left\{ \exp \left(\mathbf{m} + \frac{\mathbf{v}^2}{2} \right) \right\}.$$

Finally, we optimize with respect to v_k , for $k = 1, \dots, K$ and always set v_{K+1} as zero. Again, there are no analytical solutions and Newton's method is used for each coordinate. The first and second derivatives with respect to v_k for $k = 1, \dots, K$ are given as follows

$$\begin{aligned} \frac{\partial \tilde{F}}{\partial v_k} &= v_k^{-1} - v_k \tilde{\Sigma}_{k,k}^* - \left(\sum_{k=1}^{K+1} \mathbf{w}_k \right) \xi^{-1} \exp \left(m_k + \frac{v_k^2}{2} \right) v_k; \\ \frac{\partial^2 \tilde{F}}{\partial v_k^2} &= -v_k^{-2} - \left(\sum_{k=1}^{K+1} \mathbf{w}_k \right) \xi^{-1} \exp \left(m_k + \frac{v_k^2}{2} \right) (v_k^2 + 1). \end{aligned}$$

At each iteration of the variational EM algorithm, when we maximize the variational Gaussian lower bound $\tilde{F}(\mathbf{m}, V, \tilde{\boldsymbol{\mu}}, \tilde{\Sigma}, \xi)$ with respect to the variational parameter set (ξ, \mathbf{m}, V) , we take one step of update based on the optimization discussed above.